among imprinted disorders and the possible maternal age effect on the relative frequency.

PATIENTS AND METHODS

Patients

This study comprised 26 patients with UPD(14)pat-like phenotype (9 male patients and 17 female patients) (Table 1). Of the 26 patients, 18 patients have been reported previously; they consisted of nine sporadic patients with full UPD(14)pat,[4,5] one sporadic patient with segmental UPD(14)pat,[4] the proband of sibling cases and four sporadic patients with different patterns of microdeletions involving the unmethylated DMRs of maternal origin,[2,3] and three patients with epimutations (hypermethylations) of the two normally unmethylated DMRs of maternal origin.[2] The remaining eight patients were new sporadic cases.

Phenotypic findings of the 26 patients are summarized in Supplementary Table 1; detailed clinical features of patients 6 and 16–25 are as described previously,[2–4] and those of the eight new patients 3, 5, 10–14, and 26 are shown in Supplementary Table 2, together with those of patients 1, 2, 4, 7–9, and 15 in whom detailed phenotypes were not described in the previous report.[5] All the 26 patients were identified shortly after birth because of the unique bell-shaped thorax with coat-hanger appearance of the ribs on roentgenograms obtained because of asphyxia. Subsequent clinical analysis revealed that 25 of the 26 patients exhibited both body and placental UPD(14)pat-like phenotype, whereas the remaining one previously reported patient (patient 22) manifested body, but not placental, UPD(14)pat-like phenotype.[3] The karyotype was found to be normal in 25 patients, although cytogenetic analysis was not performed in one previously reported patient who died of respiratory failure at 2 h of age (patient 6).[4] One patient (patient 15) was conceived by *in vitro* fertilization-embryo transfer.[5] This study was approved by the Institute Review Board Committee at the National Center for Child Health and Development, and performed after obtaining written informed consent.

Analysis of underlying genetic causes in patients with UPD(14)pat-like phenotype

We sequentially performed methylation analysis, microsatellite analysis, and fluorescence *in situ* hybridization (FISH), using leukocyte genomic DNA samples and lymphocyte metaphase spreads of all the 26 patients with UPD(14)pat-like phenotype. The detailed methods were as reported previously.[2,3] In brief, methylation analysis was performed for the IG-DMR (CG4 and CG6) and the *MEG3*-DMR (CG7 and the CTCF-biding sites C and D) by combined bisulfite restriction analysis and bisulfite sequencing. Microsatellite analysis was performed for multiple loci on chromosome 14, by determining the sizes of PCR products obtained with fluorescently labeled forward primers and unlabeled reverse primers. FISH analysis was carried out for the IG-DMR and the *MEG3*-DMR using 5104-bp and 5182-bp long PCR products, respectively, together with the RP11-566I2 probe for 14q12 utilized as an internal control.

In this study, furthermore, oligonucleotide array-based comparative genomic hybridization (CGH) was also performed for the imprinted region of non-UPD(14)pat patients, using a custom-build oligo-microarray containing 12 600 probes for 14q32.2–q32.3 encompassing the imprinted region and ~10 000 reference probes for other chromosomal region (4×180K format, Design ID 032112) (Agilent Technologies, Palo Alto, CA, USA). The procedure was as described in the manufacturer's instructions.

Analysis of subtypes in patients with UPD(14)pat

UPD(14)pat subtype was determined by microsatellite analysis.[8,9] In brief, heterodisomy for at least one locus was regarded as indicative of TR- or GC-mediated UPD(14)pat (TR/GC subtype), whereas isodisomy for all the informative microsatellite loci was interpreted as indicative of MR- or PE-mediated UPD(14)pat (MR/PE subtype) (for details, see Supplementary Figure S1). Here, while heterodisomy and isodisomy for a pericentromeric region in the TR/GC subtype imply a disomic sperm generation through M1

Table 1 Summary of patients examined in this study

Patient	*Genetic cause*	*UPD(14)pat subtype*	*Maternal age at childbirth (years)*	*Paternal age at childbirth (years)*	*Remark*	*Reference*
1	UPD(14)pat	TR/GC [M1]	31	35		5
2	UPD(14)pat	TR/GC [M1]	28	29		5
3	UPD(14)pat	TR/GC [M1]	29	38		This report
4	UPD(14)pat	TR/GC [M1]	36	41		5
5	UPD(14)pat	TR/GC [M2]	30	30		This report
6	UPD(14)pat	MR/PE	42	Unknown		4,5
7	UPD(14)pat	MR/PE	31	28		5
8	UPD(14)pat	MR/PE	32	33		5
9	UPD(14)pat	MR/PE	26	35		5
10	UPD(14)pat	MR/PE	38	38		This report
11	UPD(14)pat	MR/PE	26	32		This report
12	UPD(14)pat	MR/PE	41	36		This report
13	UPD(14)pat	MR/PE	30	28		This report
14	UPD(14)pat	MR/PE	39	34		This report
15	UPD(14)pat	MR/PE	42	37	Born after IVF-ET	5
16	UPD(14)pat	MR/PE	36	36		4,5
17	UPD(14)pat-seg.	PE	27	24	Segmental isodisomy	4,5
18	Microdeletion		31	34		2
19	Microdeletion		33	36		2
20	Microdeletion		28	27		2
21	Microdeletion		27	37	IG-DMR alone	3
22	Microdeletion		25	25	*MEG3*-DMR alone	3
23	Epimutation		35	36		2
24	Epimutation		28	26		2
25	Epimutation		27	30		2
26	Epimutation		33	33		This report

Abbreviation: IVF-ET, *in vivo* fertilization-embryo transfer using parental gametes.
The microdeletions in patients 18–22 are different in size.

and M2 non-disjunction respectively,[9] such discrimination between M1 and M2 non-disjunctions is impossible for the development of a nullisomic oocyte. Furthermore, it is usually impossible to discriminate between TR and GC, although the presence of trisomic cells is specific to TR. Similarly, it is also usually impossible to discriminate between MR and PE, although identification of segmental isodisomy or mosaicism is unique to PE (PE subtype).

Analysis of parental ages

We examined parental ages at childbirth in patients of different underlying causes and different UPD(14)pat subtypes. Statistical significance of the relative frequency was examined by the Fisher's exact probability test, and that of the median age by the Mann–Whitney's *U*-test. $P<0.05$ was considered significant.

RESULTS

Analysis of underlying causes in patients with UPD(14)pat-like phenotype

For the eight new sporadic patients, methylation analysis invariably revealed hypermethylation of both DMRs, and microsatellite analysis showed UPD(14)pat in seven patients and biparentally inherited homologs of chromosome 14 in the remaining one patient (patient 26). FISH analysis for patient 26 identified two signals for the two DMRs, and subsequently performed array CGH analysis showed no evidence for genomic rearrangements (Supplementary Figure S2). Thus, patient 26 was assessed to have an epimutation affecting the two DMRs. Furthermore, the results of array CGH analysis confirmed the presence of microdeletions in patients 18–21 and the absence of a discernible microdeletion in patients 23–25 (Supplementary Figure S2) (array CGH analysis was not performed in patient 22 with a 4303-bp microdeletion[3] because of the lack of DNA sample available). Thus, together with our previous data, all the 26 patients with UPD(14)pat-like phenotype had genetic alteration involving the imprinted region on chromosome14q32.2.

Consequently, the 26 patients with UPD(14)pat-like phenotype were classified as follows: (1) 16 sporadic patients with full UPD(14)pat and 1 sporadic patient with segmental UPD(14)pat (UPD(14)pat group); (2) the proband of the sibling cases and two sporadic patients with different patterns of microdeletions involving the two DMRs, one sporadic patient with a microdeletion involving the IG-DMR alone in whom the *MEG3*-DMR was epimutated, and one patient with a microdeletion involving the *MEG3*-DMR alone (deletion group); and (3) four patients with epimutations (hypermethylations) of both DMRs (epimutation group) (Figure 1 and Table 1).

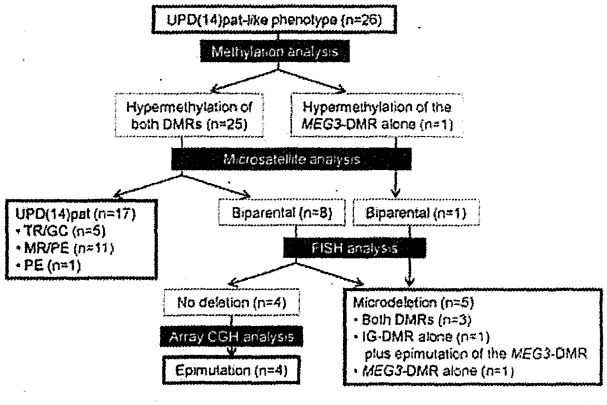

Figure 1 Classification of 26 patients with UPD(14)pat-like phenotype.

Analysis of subtypes in patients with UPD(14)pat

Heterozygosity for at least one locus indicative of TR/GC subtype was identified in five patients (patients 1–5), and the disomic pattern of pericentromeric region indicated M1 non-disjunction in patients 1–4 and M2 non-disjunction in patient 5. Full isodisomy consistent with MR/PE subtype was detected in 11 patients (patients 6–16), and segmental isodisomy unique to PE subtype was revealed in 1 patient (patient 17) (Table 1, Figure 1, and Supplementary Figure S3).

Analysis of parental ages

The distribution of parental ages at childbirth is shown in Figure 2. The advanced maternal age at childbirth (≥35 years) was predominantly observed in the MR/PE subtype of UPD(14)pat. Furthermore, while the relative frequency of aged mothers (≥35 years) did not show a significant difference between the MR/PE subtype of UPD(14)pat (6/11) and (i) other subtypes of UPD(14)pat (1/6) (P=0.159), (ii) deletion group (0/5) (P=0.057), and (iii) epimutation group (1/4) (P=0.338), it was significantly different between the MR/PE subtype and the sum of other subtypes of UPD(14)pat, deletion group, and epimutation group (2/15) (P=0.034). Similarly, while the median maternal age did not show a significant difference between the MR/PE subtype of UPD(14)pat (36 years) *vs* (i) other subtypes of UPD(14)pat (29.5 years) (P=0.118), (ii) deletion type (28 years) (P=0.088), and (iii) epimutation type (30.5 years) (P=0.295), it was significantly different between the MR/PE subtype of UPD(14)pat and the sum of other subtypes of UPD(14)pat, deletion group, and epimutation group (29 years) (P=0.045).

The paternal ages were similar irrespective of the genetic causes and the UPD(14)pat subtypes. In addition, the median paternal age was comparable between the TR/GC subtype of UPD(14)pat that postulates the production of a disomic sperm (35.0 years) and the sum of other subtypes of UPD(14)pat, deletion group, and epimutation group that assumes the production of a normal sperm (33.5 years) (P=0.322).

DISCUSSION

This study revealed that the UPD(14)pat-like phenotype was caused by UPD(14)pat in 65.4% of patients, by microdeletions in 19.2% of patients, and by epimutations in 15.4% of patients. Although the relative frequency of underlying genetic factors for the development of UPD(14)pat-like phenotype has been reported previously,[10] most data are derived from our previous publications. Thus, the present results are regarded as the updated and extended data on the relative frequency. For the relative frequency, it is notable that 25 of the 26 patients were confirmed to have normal karyotype, although chromosome analysis was not performed in patient 6. Thus, while Robertsonian translocations involving chromosome 14 is known to be a

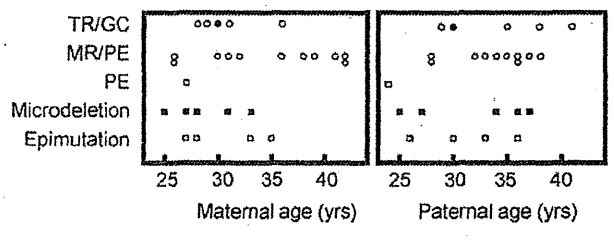

Figure 2 The distribution of parental ages at childbirth according to the underlying genetic causes for the development of UPD(14)pat-like phenotype and UPD(14)pat subtypes. Of the five plots for the TR/GC subtype, open and black circles indicate the TR/GC subtype due to non-disjunction at paternal M1 and M2, respectively.

predisposing factor for the occurrence of UPD(14)pat,[11–16] such a possible chromosomal effect has been excluded in nearly all patients examined in this study.

The relative frequency of underlying causes has also been reported in other imprinting disorders.[8,17–19] The data are summarized in Table 2 (a similar summary has also been reported recently by Hoffmann *et al*).[10] In particular, the results in patients with normal karyotype are available in Prader–Willi syndrome (PWS).[8] Furthermore, PWS is also known to be caused by UPD, microdeletions, and epimutations affecting a single imprinting region,[8,19] although Silver–Russell syndrome and Beckwith–Wiedemann syndrome (BWS) can result from perturbation of at least two imprinted regions,[17,18] and BWS and Angelman syndrome can occur as a single gene disorder.[17,19] Thus, it is notable that the relative frequency of underlying causes is quite different between patients with UPD(14)pat-like phenotype and those with PWS.[8,19] This would primarily be due to the presence of low copy repeats flanking the imprinted region on chromosome 15, because chromosomal deletions are prone to occur in regions harboring such repeat sequences.[20] Indeed, two types of microdeletions mediated by such low copy repeats account for a vast majority of microdeletions in patients with PWS,[21] whereas the microdeletions identified in patients with UPD(14)pat-like phenotype are different to each other. This would explain why microdeletions are less frequent and UPD and epimutations are more frequent in patients with UPD(14)pat-like phenotype than in those with PWS.

Advanced maternal age at childbirth was predominantly observed in the MR/PE subtype. This may imply the relevance of advanced maternal age to the development of MR-mediated UPD(14)pat, because the generation of nullisomic oocytes through M1 non-disjunction is a maternal age-dependent phenomenon.[22] Although no paternal age effect was observed, this is consistent with the previous data indicating no association of advanced paternal age with a meiotic error.[23] For the maternal age effect, however, several matters should be pointed out: (1) the number of analyzed patients is small, although it is very difficult to collect a large number of patients in this extremely rare disorder; (2) of the MR/PE subtype, the advanced maternal age is a risk factor for the generation of MR-mediated UPD(14)pat, but not for the development of PE-mediated UPD(14)pat; (3) it is impossible to discriminate between maternal age-dependent M1 non-disjunction and maternal age-independent M2 non-disjunction in the MR and GC subtypes (however, GC must be extremely rare, because it requires the concomitant occurrence of a nullisomic oocyte and a disomic sperm); (4) of the TR/GC subtype, the advanced maternal age is a risk factor for the generation of GC-mediated UPD(14)pat, but not for the development of TR-mediated UPD(14)pat; and (5) if a cryptic recombination(s) might remain undetected in some patients with apparently full isodisomy, this argues that such patients actually have TR- or GC-mediated UPD(14)pat rather than MR- or PE-mediated UPD(14)pat. Thus, further studies are required to examine the maternal age effect on the generation of MR-mediated UPD(14)pat. In addition, while a relationship is unlikely to exist between advanced maternal age and microdeletions and epimutations, this notion would also await further investigations.

Such a maternal age effect is also expected in the TR/GC subtype maternal UPDs after M1 non-disjunction, because the generation of disomic oocytes through M1 non-disjunction is also a maternal age-dependent phenomenon.[7] Indeed, such a maternal age effect has been shown for PWS patients with normal karyotype; the maternal age at childbirth was significantly higher in patients with heterodisomy for a very pericentromeric region indicative of TR/GC subtype UPD(15)mat after M1 non-disjunction than in those with other genetic causes.[8,9] For various chromosomes other than chromosome 15, furthermore, since maternal age at childbirth is higher in patients with maternal heterodisomy than in those with maternal isodisomy,[24] this would also argue for maternal age effect on the development of maternal UPDs. However, in the previous studies on maternal UPDs other than UPD(15)mat, the available data are quite insufficient to assess the maternal age effect. For example, although a relatively large number of patients with UPD(14)mat phenotype have been reported in the literature (reviewed in reference Hoffmann *et al*),[10] we could identify only six UPD(14)mat patients with normal karyotype in whom maternal age at childbirth was documented and microsatellite analysis was performed.[25–30] Furthermore, the microsatellite data are insufficient to identify the subtype of UPD(14)mat and to distinguish between M1 and M2 non-disjunction in the TR/GC subtype. Thus, while the maternal age at childbirth may be advanced in five patients with apparently TR/GC-mediated UPD(14)mat (27, 35, 37, 41, and 44 years)[25–27,29,30] (the maternal age at childbirth in the remaining one

Table 2 Relative frequency of genetic mechanisms in imprinting disorders

	UPD(14)pat-like phenotype	*BWS*	*SRS*	*AS*	*PWS*
Uniparental disomy	65.4%	16%	10%	3–5%	25% (25%)
	UPD(14)pat	UPD(11)pat (mosaic)	UPD(7)mat	UPD(15)pat	UPD(15)mat
Cryptic deletion	19.2%	Rare	—	70%	70% (72%)
Cryptic duplication	—	—	Rare	—	—
Epimutation					
Hypermethylation	15.4%	9%	—	—	2–5% (2%)
Affected DMR	IG-DMR/*MEG3*-DMR	*H19*-DMR	—	—	*SNRPN*-DMR
Hypomethylation	—	44%	>38%	2–5%	—
Affected DMR		KvDMR1	*H19*-DMR	*SNRPN*-DMR	
Gene mutation	—	5%	—	10-15%	—
Mutated gene		*CDKN1C*		*UBE3A*	
Unknown		25%	>40%	10%	
Reference	This study	17	18	19	8, 19

Abbreviations: AS, Angelman syndrome; BWS, Beckwith–Wiedemann syndrome; PWS, Prader–Willi syndrome; SRS, Silver–Russell syndrome.
Patients with abnormal karyotypes are included in BWS and AS, and not included in SRS. In PWS, the data including patients with abnormal karyotypes are shown, and those from patients with normal karyotype alone are depicted in parentheses.

patient with apparently MR/PE-mediated UPD(14)mat is 40 years),[28] the notion of a maternal age effect awaits further investigations for UPD(14)mat.

Finally, it appears to be worth pointing out that methylation analysis invariably revealed hypermethylated DMR(s) in all the 26 patients who were initially ascertained because of bell-shaped thorax with coat-hanger appearance of the ribs. This indicates that methylation analysis of the DMRs can be utilized for a screening of this condition, and that the constellation of clinical features in the UPD(14)pat-like phenotype, especially the bell-shaped thorax with coat-hanger appearance of the ribs, is highly unique to patients with UPD(14)pat-like phenotype.

In summary, this study confirms the relative frequency of underlying genetic causes for the UPD(14)pat phenotype and reveals the relative frequency of UPD(14)pat subtypes. Furthermore, the results emphasize the difference in the relative frequency of underlying genetic causes among imprinted disorders, and may support a possible maternal age effect on the generation of the nullisomic oocyte mediated UPD(14)pat. Further studies will permit a more precise assessment on these matters.

CONFLICT OF INTEREST

The authors declare no conflict of interest.

ACKNOWLEDGEMENTS

We thank Drs Kenji Kurosawa, Michiko Hayashidani, Toshio Takeuchi, Shinya Tanaka, Mika Noguch, Kouji Masumoto, Takeshi Utsunomiya, Yumiko Komatsu, Hirofumi Ohashi, Maureen J O'Sullivan, Andrew J Green, Yoshiyuki Watabe, Tsuyako Iwai, Hitoshi Kawato, Miho Torikai, Akiko Yamamoto, Nobuhiro Suzumori, Makoto Kuwajima, Hiroshi Yoshihashi, Yoriko Watanabe, and Jin Nishimura for material sampling and phenotype assessment. This work was supported by Grants for Research on Intractable Diseases (H22-161) and for Health Research on Children, Youth and Families (H21-005) from the Ministry of Health, Labor and Welfare, by Grants-in-Aid for Scientific Research (A) (22249010) and (B) (21028026) from the Japan Society for the Promotion of Science (JSPS), by Grants from Takeda Science Foundation and from Kanehara Foundation, and by the Grant for National Center for Child Health and Development (23A-1).

1 da Rocha ST, Edwards CA, Ito M, Ogata T, Ferguson-Smith AC: Genomic imprinting at the mammalian Dlk1-Dio3 domain. *Trends Genet* 2008; **24**: 306–316.
2 Kagami M, Sekita Y, Nishimura G *et al*: Deletions and epimutations affecting the human 14q32.2 imprinted region in individuals with paternal and maternal upd(14)-like phenotypes. *Nat Genet* 2008; **40**: 237–242.
3 Kagami M, O'Sullivan MJ, Green AJ *et al*: The IG-DMR and the MEG3-DMR at human chromosome 14q32.2: hierarchical interaction and distinct functional properties as imprinting control centers. *PLoS Genet* 2010; **6**: e1000992.
4 Kagami M, Nishimura G, Okuyama T *et al*: Segmental and full paternal isodisomy for chromosome 14 in three patients: narrowing the critical region and implication for the clinical features. *Am J Med Genet A* 2005; **138A**: 127–132.
5 Kagami M, Yamazawa K, Matsubara K, Matsuo N, Ogata T: Placentomegaly in paternal uniparental disomy for human chromosome 14. *Placenta* 2008; **29**: 760–761.
6 Shaffer LG, Agan N, Goldberg JD, Ledbetter DH, Longshore JW, Cassidy SB: American College of Medical Genetics statement of diagnostic testing for uniparental disomy. *Genet Med* 2001; **3**: 206–211.
7 Jones KT: Meiosis in oocytes: predisposition to aneuploidy and its increased incidence with age. *Hum Reprod Update* 2008; **14**: 143–158.
8 Matsubara K, Murakami N, Nagai T, Ogata T: Maternal age effect on the development of Prader-Willi syndrome resulting from upd(15)mat through meiosis 1 errors. *J Hum Genet* 2011; **56**: 566–571.
9 Robinson WP, Christian SL, Kuchinka BD *et al*: Somatic segregation errors predominantly contribute to the gain or loss of a paternal chromosome leading to uniparental disomy for chromosome 15. *Clin Genet* 2000; **57**: 349–358.
10 Hoffmann K, Heller R: Uniparental disomies 7 and 14. *Best Pract Res Clin Endocrinol Metab* 2011; **25**: 77–100.
11 Wang JC, Passage MB, Yen PH, Shapiro LJ, Mohandas TK: Uniparental heterodisomy for chromosome 14 in a phenotypically abnormal familial balanced 13/14 Robertsonian translocation carrier. *Am J Hum Genet* 1991; **48**: 1069–1074.
12 Papenhausen PR, Mueller OT, Johnson VP, Sutcliffe M, Diamond TM, Kousseff BG: Uniparental isodisomy of chromosome 14 in two cases: an abnormal child and a normal adult. *Am J Med Genet* 1995; **59**: 271–275.
13 Cotter PD, Kaffe S, McCurdy LD, Jhaveri M, Willner JP, Hirschhorn K: Paternal uniparental disomy for chromosome 14: a case report and review. *Am J Med Genet* 1997; **70**: 74–79.
14 Yano S, Li L, Owen S, Wu S, Tran T: A further delineation of the paternal uniparental disomy (UPD14): the fifth reported liveborn case. *Am J Hum Genet* 2001; **69** (Suppl): A739.
15 Kurosawa K, Sasaki H, Sato Y *et al*: Paternal UPD14 is responsible for a distinctive malformation complex. *Am J Med Genet A* 2002; **110**: 268–272.
16 McGowan KD, Weiser JJ, Horwitz J *et al*: The importance of investigating for uniparental disomy in prenatally identified balanced acrocentric rearrangements. *Prenat Diagn* 2002; **22**: 141–143.
17 Sasaki K, Soejima H, Higashimoto K *et al*: Japanese and North American/European patients with Beckwith-Wiedemann syndrome have different frequencies of some epigenetic and genetic alterations. *Eur J Hum Genet* 2007; **15**: 1205–1210.
18 Eggermann T: Epigenetic regulation of growth: lessons from Silver-Russell syndrome. *Endocr Dev* 2009; **14**: 10–19.
19 Gurrieri F, Accadia M: Genetic imprinting: the paradigm of Prader-Willi and Angelman syndromes. *Endocr Dev* 2009; **14**: 20–28.
20 Pujana MA, Nadal M, Guitart M, Armengol L, Gratacos M, Estivill X: Human chromosome 15q11-q14 regions of rearrangements contain clusters of LCR15 duplicons. *Eur J Hum Genet* 2002; **10**: 26–35.
21 Varela MC, Kok F, Setian N, Kim CA, Koiffmann CP: Impact of molecular mechanisms, including deletion size, on Prader-Willi syndrome phenotype: study of 75 patients. *Clin Genet* 2005; **67**: 47–52.
22 Pellestor F, Andreo B, Anahory T, Hamamah S: The occurrence of aneuploidy in human: lessons from the cytogenetic studies of human oocytes. *Eur J Med Genet* 2006; **49**: 103–116.
23 Sloter E, Nath J, Eskenazi B, Wyrobek AJ: Effects of male age on the frequencies of germinal and heritable chromosomal abnormalities in humans and rodents. *Fertil Steril* 2004; **81**: 925–943.
24 Kotzot D: Advanced parental age in maternal uniparental disomy (UPD): implications for the mechanism of formation. *Eur J Hum Genet* 2004; **12**: 343–346.
25 Fokstuen S, Ginsburg C, Zachmann M, Schinzel A: Maternal uniparental disomy 14 as a cause of intrauterine growth retardation and early onset of puberty. *J Pediatr* 1999; **134**: 689–695.
26 Hordijk R, Wierenga H, Scheffer H, Leegte B, Hofstra RM, Stolte-Dijkstra I: Maternal uniparental disomy for chromosome 14 in a boy with a normal karyotype. *J Med Genet* 1999; **36**: 782–785.
27 Sanlaville D, Aubry MC, Dumez Y *et al*: Maternal uniparental heterodisomy of chromosome 14: chromosomal mechanism and clinical follow up. *J Med Genet* 2000; **37**: 525–528.
28 Towner DR, Shaffer LG, Yang SP, Walgenbach DD: Confined placental mosaicism for trisomy 14 and maternal uniparental disomy in association with elevated second trimester maternal serum human chorionic gonadotrophin and third trimester fetal growth restriction. *Prenat Diagn* 2001; **21**: 395–398.
29 Aretz S, Raff R, Woelfle J *et al*: Maternal uniparental disomy 14 in a 15-year-old boy with normal karyotype and no evidence of precocious puberty. *Am J Med Genet A* 2005; **135**: 336–338.
30 Mitter D, Buiting K, von Eggeling F *et al*: Is there a higher incidence of maternal uniparental disomy 14 [upd(14)mat]? Detection of 10 new patients by methylation-specific PCR. *Am J Med Genet A* 2006; **140**: 2039–2049.

Supplementary Information accompanies the paper on European Journal of Human Genetics website (http://www.nature.com/ejhg)

RESEARCH LETTER

AMERICAN JOURNAL OF medical genetics PART A

Mosaic upd(7)mat in a Patient With Silver–Russell Syndrome

Tomoko Fuke-Sato,[1,2] Kazuki Yamazawa,[1] Kazuhiko Nakabayashi,[3] Keiko Matsubara,[1] Kentaro Matsuoka,[4] Tomonobu Hasegawa,[2] Kazushige Dobashi,[5] and Tsutomu Ogata[1,6]*

[1]Department of Molecular Endocrinology, National Research Institute for Child Health and Development, Tokyo, Japan

[2]Department of Pediatrics, Keio University School of Medicine, Tokyo, Japan

[3]Department of Maternal-Fetal Biology, National Research Institute for Child Health and Development, Tokyo, Japan

[4]Division of Pathology, National Medical Center for Children and Mothers, Tokyo, Japan

[5]Department of Pediatrics, Showa University School of Medicine, Tokyo, Japan

[6]Department of Pediatrics, Hamamatsu University School of Medicine, Hamamatsu, Japan

Received 10 March 2011; Accepted 9 November 2011

TO THE EDITOR:

Silver–Russell syndrome (SRS) is a congenital developmental disorder characterized by pre- and post-natal growth failure, relative macrocephaly, triangular face, hemihypotrophy, and 5th finger clinodactyly [Russell, 1954; Silver et al., 1953]. Recent studies have shown that hypomethylation (epimutation) of the paternally derived differentially methylated region (DMR) in the upstream of *H19* (*H19*-DMR) on chromosome 11p15 and maternal uniparental disomy for chromosome 7 (upd(7)mat) account for ~45% and ~5–10% of SRS patients, respectively [Eggermann, 2010; Binder et al., 2011]. Furthermore, consistent with the involvement of imprinted genes in both body and placental growth [for review, Coan et al., 2005], epimutations of the *H19*-DMR and upd(7)mat are known to result in placental hypoplasia [Yamazawa et al., 2008a,b]. Here, we report on a Japanese boy with mosaic upd(7)mat who was identified through genetic screenings in 120 patients with SRS-like phenotype.

This Japanese boy was conceived naturally to a 41-year-old father and a 36-year-old mother. The parents were non-consanguineous and healthy. The paternal height was 165 cm (−0.9 SD), and the maternal height 155 cm (−0.6 SD).

At 35 weeks of gestation, he was delivered by a cesarean because of fetal distress. At birth, his length was 37.4 cm (−3.1 SD), his weight 1.28 kg (−3.1 SD), and his head circumference 29.0 cm (−1.3 SD). The placenta weighed 400 g (−0.6 SD [Kagami et al., 2008]). Shortly after birth, he was found to have ventricular septal defect, hydronephrosis, and abnormal external genitalia (hypospadias, bifid scrotum, and bilateral cryptorchidism). He received orchidopexy at $1^{10}/_{12}$ years of age and genitoplasty at $2^{4}/_{12}$ years of age. He exhibited feeding difficulty and speech delay.

At $5^{1}/_{12}$ years of age, he was referred because of short stature. His height was 87.9 cm (−4.3 SD), weight was 10.4 kg (−2.9 SD), and his head circumference 49.0 cm (−0.7 SD). Physical examination showed relative macrocephaly, abnormal teeth, 5th finger clinodactyly, and underdeveloped muscles. There was no hemihypotrophy. Endocrine studies for short stature yielded normal results, as did radiological examinations. His karyotype was 46,XY in all the 50 lymphocytes examined. He was clinically diagnosed as having SRS, and molecular studies were performed after obtaining the approval from the Institutional Review Board Committee at National Center for Child Health and Development and the written informed consent from the parents.

We first performed methylation analysis of the *MEST*-DMR on chromosome 7q32.2 using leukocyte genomic DNA by the previously described methods [Yamazawa et al., 2008b], because this patient showed relatively mild SRS-phenotype with speech delay

How to Cite this Article:
Fuke-Sato T, Yamazawa K, Nakabayashi K, Matsubara K, Matsuoka K, Hasegawa T, Dobashi K, Ogata T. 2012. Mosaic upd(7)mat in a patient with Silver–Russell syndrome. Am J Med Genet Part A 158A:465–468.

Grant sponsor: Japan Society for the Promotion of Science (JSPS); Grant number: 22249010; Grant sponsor: Ministry of Health, Labor and Welfare; Grant number: H21-005; Grant sponsor: Grant of National Center for Child Health and Development; Grant number: 23A-1.

*Correspondence to:
Tsutomu Ogata, M.D., Department of Pediatrics, Hamamatsu University School of Medicine, Hamamatsu 431-3192, Japan.
E-mail: tomogata@hama-med.ac.jp

Published online 13 January 2012 in Wiley Online Library (wileyonlinelibrary.com).
DOI 10.1002/ajmg.a.34404

and feeding difficulty characteristic of upd(7)mat [Hitchins et al., 2001; Kotzot, 2008]. The methylation analysis showed a major peak for methylated clones and a minor peak for unmethylated clones in this patient (Fig. 1A). We also examined the *H19*-DMR and other multiple DMRs on various chromosomes by the bio-COBRA (combined bisulfite restriction analysis) method, as reported previously [Yamazawa et al., 2010]. The *GRB10*-DMR on chromosome 7p12.1 and the *PEG10*-DMR on chromosome 7q21.3 exhibited skewed methylation patterns consistent with the predominance of maternally derived clones, as did the *MEST*-DMR (Fig. 1B). By

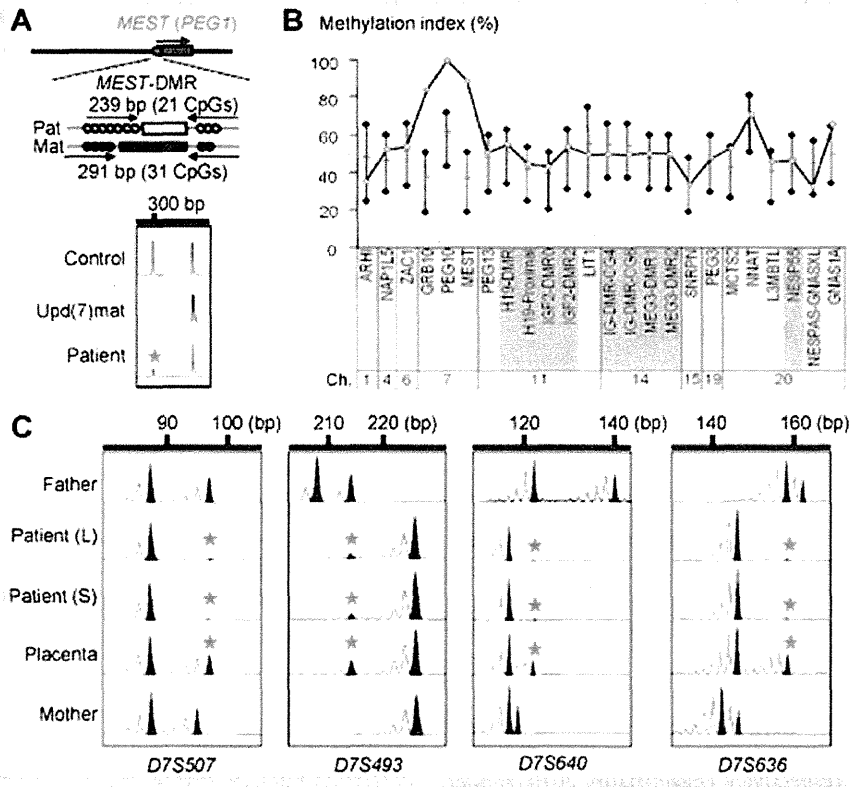

FIG. 1. Representative molecular results. A: Methylation analysis for the *MEST*-DMR. The methylated and unmethylated allele-specific primers were designed to yield PCR products of different sizes, and the PCR products were visualized on the 2100 Bioanalyzer (Agilent, Santa Clara, CA). Both methylated and unmethylated alleles are amplified in a control subject, and the methylated allele only is identified in a previously reported patient with upd(7)mat [Yamazawa et al., 2008b]. In this patient, a major peak for the methylated allele and a minor peak for the unmethylated allele (a red asterisk) are delineated. B: Methylation indices of 24 DMRs examined by the bio-COBRA. The PCR products were digested with methylation sensitive restriction enzymes, and the methylation indices (the ratios of methylated clones) were calculated using peak heights of digested and undigested fragments on the 2100 Bioanalyzer using 2100 expert software. The black vertical bars indicate the reference data in 20 normal control subjects (maximum – minimum). The DMRs highlighted in blue and pink are methylated after paternal and maternal transmissions, respectively. C: Microsatellite analysis. Major peaks of maternal origin and minor peaks of paternal origin (red asterisks) are identified in this patient. The minor peaks of paternal origin are more obvious in the placenta than in the leukocytes (L) and salivary cells (S). Calculation of the mosaic ratio using the *D7S507* data, under the assumption of no trisomic cells. For this locus, the patient is considered to be heterozygous with the major 87 bp peak of maternal origin and a minor 97 bp peak of paternal origin. The father is also heterozygous with the two peaks of the same sizes, and the area under curve (AUC) is larger for the short 87 bp peak than for the long 97 bp peak. This unequal amplification is consistent with short products being more easily amplified than long products. In this patient, the AUC ratio between the major 87 bp peak and the minor 97 bp peak is obtained as 1.0:0.043 for leukocytes, 1.0:0.044 for salivary cells, and 1.0:0.803 in placental tissue, after compensation of the unequal amplification between the two peaks using the paternal data. Here, let "XL" represent the frequency of the upid(7)mat cells in leukocytes (thus, (1 – XL) denotes the frequency of normal cells in leukocytes). Then, the paternally derived 97 bp peak is generated by one paternally derived chromosome in the normal cells, that is, (1 – XL), and the maternally derived 87 bp peak is formed by the products from two maternally derived homologous chromosomes in the upid(7)mat cells and one maternally derived chromosome in the normal cells, that is, {2XL + (1 – XL)} = (XL + 1). Thus, the AUC ratio between the two peaks is represented as (XL + 1):(1 – XL) = 1.0:0.043, and "XL" is calculated as 0.92 (92%). Similarly, when "XS" and "XP" represent the frequency of the upid(7)mat cells in salivary cells and placental tissue, respectively, "XS" is obtained as 0.91 (91%) and "XP" as 0.11 (11%). Furthermore, when "XB" represents the frequency of the upid(7)mat cells in buccal epithelium cells, "XB" is obtained as 0.91 (91%), on the basis of the previous report that salivary cells comprises ~40% of buccal epithelium cells and ~60% of leukocytes [Thiede et al., 2000].

TABLE I. The Results of Microsatellite Analysis

Locus	Position	Father	Patient (L)	Patient (S)	Placenta	Mother	Assessment
D7S517	7p22.2	254/258	(254)/258	(254)/258	(254)/258	256/258	Maternal Iso-D[a]/biparental
D7S507	7p15–21	87/97	87/(97)	87/(97)	87/(97)	87/95	Maternal Iso-D[a]/biparental
D7S493	7p15.3	208/214	(214)/226	(214)/226	(214)/226	226	Maternal D[b]/biparental
D7S484	7p14–15	96/100	(96)/98	(96)/98	(96)/98	98/100	Maternal Iso-D/biparental
D7S502	7q11.12	298	294/(298)	294/(298)	294/(298)	294/304	Maternal Iso-D/biparental
D7S669	7q11.2	116/126	(116)/124	(116)/124	(116)/124	124	Maternal D[b]/biparental
D7S515	7q21–22	169/173	171/(173)	171/(173)	171/(173)	169/171	Maternal Iso-D/biparental
D7S640	7q21.1–31.2	122/140	116/(122)	116/(122)	116/(122)	116/118	Maternal Iso-D/biparental
D7S684	7q34	169/179	177/(179)	177/(179)	177/(179)	177/179	Not informative
D7S636	7q35–36	158/162	146/(158)	146/(158)	146/(158)	142/146	Maternal Iso-D/biparental
D7S798	7q36	73/79	(79)/83	(79)/83	(79)/83	73/83	Maternal Iso-D/biparental

L, leukocytes; S, salivary cells; D, disomy.
The Arabic numbers denote the PCR product sizes in bp.
The minor peaks are indicated in parentheses.
[a]On the basis of the results of other informative loci, the major peaks are considered to be of maternal origin.
[b]Because of the maternal homozygosity, disomic status (isodisomy or heterodisomy) is unknown for these loci.

contrast, other DMRs including the *H19*-DMR showed normal methylation patterns.

We next performed microsatellite analysis for 11 loci on various parts of chromosome 7, using genomic DNA from leukocytes of the patient and the parents, from salivary cells of the patient, and from formalin-fixed and paraffin-embedded placental tissue. Major peaks consistent with maternal uniparental isodisomy and minor peaks of paternal origin were unequivocally identified for *D7S484*, *D7S502*, *D7S515*, *D7S640*, *D7S636*, and *D7S798*; furthermore, similar patterns were also detected for *D7S517*, *D7S507*, *D7S669*, and *D7S493*, although the results were not informative for *D7S684* (Fig. 1C and Table I). The minor peaks of paternal origin were similar between leukocytes and salivary cells and more evident in placental tissue. These findings, together with the normal karyotype in lymphocytes, indicated mosaic full maternal isodisomy for chromosome 7 (upid(7)mat) in this patient. Furthermore, since such a condition is frequently associated with mosaicism for trisomy 7 [Petit et al., 2011], we performed fluorescence in situ hybridization (FISH) analysis for stocked lymphocyte pellets, using a CEP7 probe for *D7Z1* (Abbott Laboratories, Abbott Park, IL). The FISH analysis identified two normal signals in 995 of 1,000 interphase nuclei examined, with no trace of trisomic nuclei; while a single signal was delineated in the remaining five nuclei, this was regarded as a false-positive finding. Thus, assuming no trisomic cells, the frequency of the full upid(7)mat cells was calculated as 92% in leukocytes, using the results of *D7S507* (Fig. 1C). In addition, similarly assuming no trisomic cells in other tissues, the frequency of the full upid(7)mat cells was calculated as 91% salivary cells (and in buccal cells) and 11% in placental tissue, although we could not perform FISH analysis in buccal cells and placental cells.

These results imply that this patient had an abnormal cell lineage with full upid(7)mat and a normal cell lineage with biparentally inherited chromosome 7 homologs at least in lymphocytes, and these had no trisomy 7. It is likely that mitotic non-disjunction and subsequent trisomy rescue (loss of the paternally derived chromosome 7 from a trisomic cell) took place in the post-zygotic developmental stage, resulting in the production of the mosaic full upid(7)mat (Fig. 2). While full upid(7)mat can also be produced by monosomy rescue (duplication of a single maternally derived chromosome 7 in a zygote), this mechanism is predicted to cause non-mosaic rather than mosaic upid(7)mat [Miozzo et al., 2001]. Although it remains to be clarified why trisomic cells mediating the production of full upid(7)mat cells were apparently absent in lymphocytes of this patient, there might be a negative selection against lymphocytes with trisomy 7.

However, the presence or absence of demonstrable trisomic cells was studied only in lymphocytes. In this regard, trisomic cells have been identified more frequently in skin fibroblasts and amniocytes than in blood cells in patients with mosaic trisomy 7 [Chen et al., 2010; Petit et al., 2011], and they are usually more frequently detected in the placental tissue than in the body tissue, as has been demonstrated by confined placental trisomy [Kalousek et al., 1991]. These findings would argue for the possible presence of trisomic cells in several tissues including placenta of this patient.

The full upid(7)mat cells were assessed to account for the majority of the leukocytes and salivary cells (buccal cells) and the minority of the placental tissue, under the assumption of no

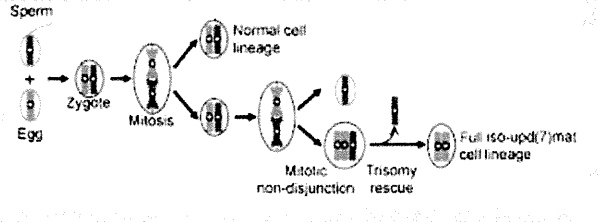

FIG. 2. Schematic representation of the generation of the mosaic upid(7)mat. The maternally and paternally derived chromosome 7 homologs are shown in red and blue, respectively. In this figure, mitotic non-disjunction is assumed at the second mitosis.

trisomic cells. In this regard, if trisomic cells may be present in a certain fraction of buccal cells and placental tissue, the full upid(7)mat cells would still account for a relatively major fraction of buccal cells and a relatively minor fraction of the placental cells. While such a variation in the frequency of the full upid(7)mat cells among different tissues would primarily be a stochastic event, it should be pointed out that human genetic studies are usually performed for leukocytes. Indeed, if the upid(7)mat cells were barely present in leukocytes, the mosaic upid(7)mat would not have been detected. Such a bias in human studies would more or less be relevant to the relative predominance of the full upid(7)mat cells in leukocytes.

Two findings are noteworthy with regard to clinical features of this patient. First, this patient had relatively mild SRS phenotype with speech delay and feeding difficulty. Since such clinical features are grossly consistent with those of patients with upd(7)mat [Hitchins et al., 2001; Kotzot, 2008], it is inferred that the upid(7)mat cells accounted for a considerable fraction of body cells relevant to the development of SRS phenotype. Second, the placental size remained within the normal range. This would be consistent with the relative paucity of the upid(7)mat cells in the placenta.

In summary, we observed mosaic upid(7)mat in a patient with SRS. Further studies will identify mosaic upd(7)mat with or without demonstrable trisomy 7 in patients with relatively mild SRS-like phenotype.

ACKNOWLEDGMENTS

This work was supported by the Grant-in-Aid for Scientific Research (A) (22249010) from the Japan Society for the Promotion of Science (JSPS), by the Grants for Health Research on Children, Youth, and Families (H21-005) from the Ministry of Health, Labor and Welfare, and by the Grant of National Center for Child Health and Development (23A-1).

REFERENCES

Binder G, Begemann M, Eggermann T, Kannenberg K. 2011. Silver-Russell syndrome. Best Pract Res Clin Endocrinol Metab 25:153–160.

Chen CP, Su YN, Chern SR, Hwu YM, Lin SP, Hsu CH, Tsai FJ, Wang TY, Wu PC, Lee CC, Chen YT, Chen LF, Wang W. 2010. Mosaic trisomy 7 at amniocentesis: Prenatal diagnosis and molecular genetic analyses. Taiwan J Obstet Gynecol 49:333–340.

Coan PM, Burton GJ, Ferguson-Smith AC. 2005. Imprinted genes in the placenta: A review. Placenta 26:S10–S20.

Eggermann T. 2010. Russell–Silver syndrome. Am J Med Genet Part C 154C:355–364.

Hitchins MP, Stanier P, Preece MA, Moore GE. 2001. Silver-Russell syndrome: A dissection of the genetic aetiology and candidate chromosomal regions. J Med Genet 38:810–819.

Kagami M, Yamazawa K, Matsubara K, Matsuo N, Ogata T. 2008. Placentomegaly in paternal uniparental disomy for human chromosome 14. Placenta 29:760–761.

Kalousek DK, Howard-Peebles PN, Olson SB, Barrett IJ, Dorfmann A, Black SH, Schulman JD, Wilson RD. 1991. Confirmation of CVS mosaicism in term placentae and high frequency of intrauterine growth retardation association with confined placental mosaicism. Prenat Diagn 11:743–750.

Kotzot D. 2008. Maternal uniparental disomy 7 and Silver–Russell syndrome—Clinical update and comparison with other subgroups. Eur J Med Genet 51:444–451.

Miozzo M, Grati FR, Bulfamante G, Rossella F, Cribiù M, Radaelli T, Cassani B, Persico T, Cetin I, Pardi G, Simoni G. 2011. Post-zygotic origin of complete maternal chromosome 7 isodisomy and consequent loss of placental *PEG1/MEST* expression. Placenta 22:813–821.

Petit F, Holder-Espinasse M, Duban-Bedu B, Bouquillon S, Boute-Benejean O, Bazin A, Rouland V, Manouvrier-Hanu S, Delobel B. 2011. Trisomy 7 mosaicism prenatally misdiagnosed and maternal uniparental disomy in a child with pigmentary mosaicism and Russell–Silver syndrome. Clin Genet [Epub ahead of print], PHID: 21204802.

Russell A. 1954. A syndrome of intra-uterine dwarfism recognizable at birth with cranio-facial dysostosis, disproportionately short arms and other anomalies. Proc R Soc Med 47:1040–1044.

Silver HK, Kiyasu W, George J, Deamer WC. 1953. Syndrome of congenital hemihypertrophy, shortness of stature, and elevated urinary gonadotrophins. Pediatrics 12:368–375.

Thiede C, Prange-Krex G, Freiberg-Richter J, Bornhäuser M, Ehninger G. 2000. Buccal swabs but not mouthwash samples can be used to obtain pretransplant DNA fingerprints from recipients of allogeneic bone marrow transplants. Bone Marrow Transplant 25:575–577.

Yamazawa K, Kagami M, Nagai T, Kondoh T, Onigata K, Maeyama K, Hasegawa T, Hasegawa Y, Yamazaki T, Mizuno S, Miyoshi Y, Miyagawa S, Horikawa R, Matsuoka K, Ogata T. 2008a. Molecular and clinical findings and their correlations in Silver-Russell syndrome: Implications for a positive role of IGF2 in growth determination and differential imprinting regulation of the *IGF2-H19* domain in bodies and placentas. J Mol Med 86:1171–1181.

Yamazawa K, Kagami M, Ogawa M, Horikawa R, Ogata T. 2008b. Placental hypoplasia in maternal uniparental disomy for chromosome 7. Am J Med Genet Part A 146A:514–516.

Yamazawa K, Nakabayashi K, Kagami M, Sato T, Saitoh S, Horikawa R, Hizuka N, Ogata T. 2010. Parthenogenetic chimaerism/mosaicism with a Silver-Russell syndrome-like phenotype. J Med Genet 47:782–785.

Papers in Press. Published January 24, 2012 as doi:10.1373/clinchem.2011.173286
The latest version is at http://hwmaint.clinchem.org/cgi/doi/10.1373/clinchem.2011.173286

Clinical Chemistry 58:4
000–000 (2012)

Two-Step Biochemical Differential Diagnosis of Classic 21-Hydroxylase Deficiency and Cytochrome P450 Oxidoreductase Deficiency in Japanese Infants by GC-MS Measurement of Urinary Pregnanetriolone/ Tetrahydroxycortisone Ratio and 11β-Hydroxyandrosterone

Yuhei Koyama,[1,2] Keiko Homma,[3] Maki Fukami,[4] Masayuki Miwa,[5] Kazushige Ikeda,[5] Tsutomu Ogata,[4] Tomonobu Hasegawa,[5*] and Mitsuru Murata[1]

BACKGROUND: The clinical differential diagnosis of classic 21-hydroxylase deficiency (C21OHD) and cytochrome P450 oxidoreductase deficiency (PORD) is sometimes difficult, since both deficiencies can have similar phenotypes and high blood concentrations of 17α-hydroxyprogesterone (17OHP). The objective of this study was to identify biochemical markers for the differential diagnosis of C21OHD, PORD, and transient hyper 17α-hydroxyprogesteronemia (TH17OHP) in Japanese newborns. We established a 2-step biochemical differential diagnosis of C21OHD and PORD.

METHODS: We recruited 29 infants with C21OHD, 9 with PORD, 67 with TH17OHP, and 1341 control infants. All were Japanese and between 0 and 180 days old; none received glucocorticoid treatment before urine sampling. We measured urinary pregnanetriolone (Ptl), the cortisol metabolites 5α- and 5β-tetrahydrocortisone (sum of these metabolites termed THEs), and metabolites of 3 steroids, namely dehydroepiandrosterone, androstenedione (AD4), and 11β-hydroxyandrostenedione (11OHAD4) by GC-MS.

RESULTS: At a cutoff of 0.020, the ratio of Ptl to THEs differentiated C21OHD and PORD from TH17OHP and controls with no overlap. Among metabolites of DHEA, AD4, and 11OHAD4, only 11β-hydroxyandrosterone (11HA), a metabolite of 11OHAD4, showed no overlap between C21OHD and PORD at a cutoff of 0.35 mg/g creatinine.

CONCLUSIONS: A specific cutoff for the ratio of Ptl to THEs can differentiate C21OHD and PORD from TH17OHP and controls. Additionally, the use of a specific cutoff of 11HA can distinguish between C21OHD and PORD.

Classic 21-hydroxylase deficiency (C21OHD)[6] is the most common form of congenital adrenal hyperplasia, which is transmitted as an autosomal recessive trait. C21OHD is caused by mutations of *CYP21A2* (cytochrome P450, family 21, subfamily A, polypeptide 2)[7] encoding 21-hydroxylase, which catalyzes steroid hydroxylation at C21 (Fig. 1) *(1)*. C21OHD shows adrenal insufficiency, disorders of sex development in 46,XX, and increased serum 17α-hydroxyprogesterone (17OHP). Cytochrome P450 oxidoreductase (POR) deficiency (PORD) is a recently established form of congenital adrenal hyperplasia that is also transmitted as an autosomal recessive trait. PORD is caused by mutations of *POR* encoding POR, which transfers electrons to microsomal P450 enzymes such as 17-hydroxylase/17,20-lyase, 21-hydroxylase, and aromatase (Fig. 1) *(2)*. PORD shows adrenal dysfunction,

[1] Department of Laboratory Medicine and [5] Department of Pediatrics, Keio University School of Medicine, Tokyo, Japan; [2] Mitsubishi Chemical Medience Co., Tokyo, Japan; [3] Keio University Hospital Central Clinical Laboratories, Tokyo, Japan; [4] Department of Endocrinology and Metabolism, National Center for Child Health and Development, Tokyo, Japan.
* Address correspondence to this author at: Department of Pediatrics, Keio University School of Medicine, 35 Shinanomachi, Shinjuku-ku, Tokyo, 160-8582, Japan; Fax +81-3-5379-1978; e-mail thaseg@a6.keio.jp.
Received August 3, 2011; accepted January 5, 2012.
Previously published online at DOI: 10.1373/clinchem.2011.173286

[6] Nonstandard abbreviations: C21OHD, classic 21-hydroxylase deficiency; 17OHP, 17α-hydroxyprogesterone; POR, cytochrome P450 oxidoreductase; PORD, POR deficiency; TH17OHP, transient hyper 17OHPnemia; Ptl, pregnanetriolone; 21DOF, 21-deoxycortisol; 11HA, 11β-hydroxyandrosterone; PD, pregnanediol; GC-MS-SIM, GC-MS/selected ion monitoring; THE, tetrahydrocortisone; DHEA, dehydroepiandrosterone; AD4, androstenedione; 11OHAD4, 11β-hydroxyandrostenedione.
[7] Human genes: *CYP21A2*, cytochrome P450, family 21, subfamily A, polypeptide 2; *POR*, P450 (cytochrome) oxidoreductase.

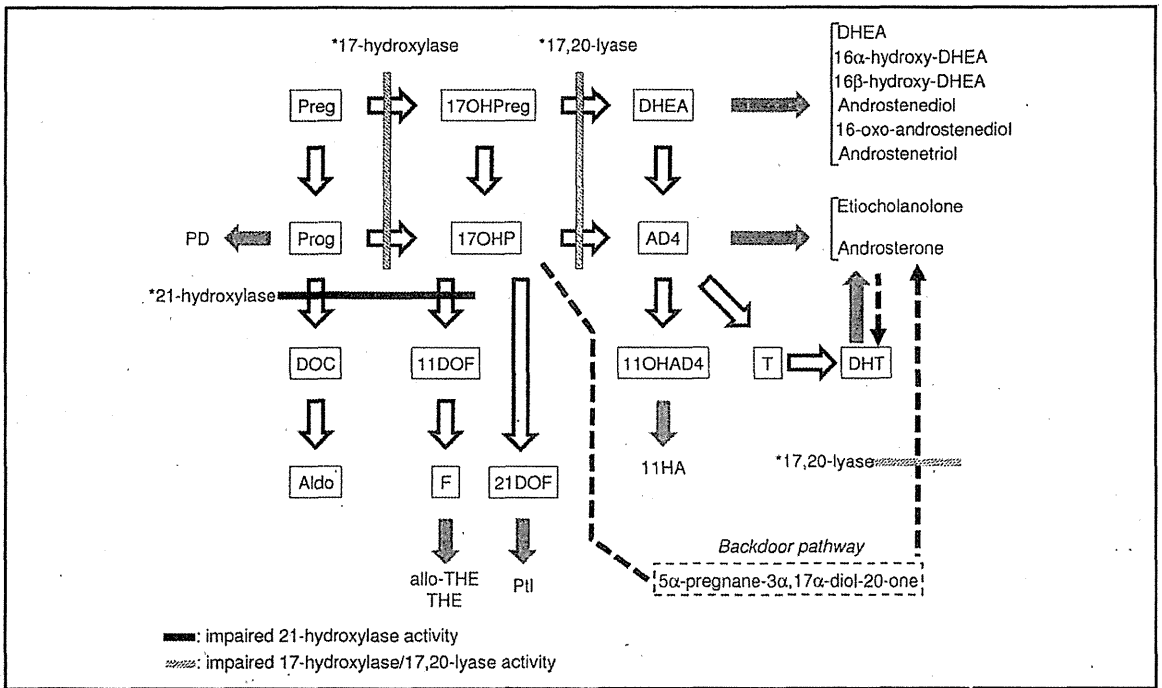

Fig. 1. Steroid metabolic map. *: enzymes that work with POR.

Preg, Pregnenolone; Prog, progesterone; DOC, deoxycorticosterone; Aldo, aldosterone; 17OHPreg, 17α-hydroxypregnenolone; 11DOF, 11-deoxycortisol; F, cortisol; T, testosterone; DHT, dihydrotestosterone. Open arrow, steroid synthesis; closed arrow, steroid metabolism; dashed arrow, backdoor pathway; open square, steroids in blood. Note that both 21-hydroxylase and 17-hydroxylase/17,20-lyase activities are reduced in PORD whereas only 21-hydroxylase is reduced in C21OHD.

disorders of sex development in 46,XX and 46,XY, skeletal dysplasia, maternal virilization during pregnancy, and increased serum 17OHP. In addition to increased concentrations of 17OHP, clinical manifestations of C21OHD and PORD can be similar, leading to difficulty in differential diagnosis *(3, 4)*. We previously reported the biochemical differential diagnosis of C21OHD from transient hyper 17OHPnemia (TH17OHP) and controls in term and preterm neonates by measuring urinary pregnanetriolone (Ptl), which was a final metabolite of 21-deoxycortisol (21DOF) *(5)*. Shackleton et al. *(6)* reported biochemical differential diagnosis of PORD from controls by a distinctive steroid excretion pattern, namely low urinary metabolites of cortisol and androgens and high metabolites of pregnenolone and progesterone. We reported that PORD had high urinary Ptl concentrations and that the ratio of 11β-hydroxyandrosterone (11HA) to pregnanediol (PD) could differentiate PORD from C21OHD in 3 infants between the ages of 1 and 3 months *(3)*. However, no cutoff for urinary steroid metabolites has been reported at any age for distinguishing between C21OHD and PORD. In our laboratory, the measurement of PD in newborns is sometimes problematic owing to unknown interferences, and we have not been able to calculate the ratio of 11HA to PD for the differential diagnosis of C21OHD and PORD.

The objective of this study was to identify biochemical markers for the differential diagnosis of C21OHD, PORD, and TH17OHP and to set the cutoff in Japanese infants <6 months old, the period during which most patients with C21OHD or PORD are diagnosed *(7)*. We paid attention to 21-hydroxylase and 17,20-lyase activities since, theoretically, the former enzymatic activity is impaired in both C21OHD and PORD and the latter is impaired in PORD but not C21OHD.

Materials and Methods

All legal guardians gave written informed consent, and the study was approved by the institutional review board committee at Keio University Hospital. We recruited 29 infants with C21OHD, 9 with PORD, 67 with TH17OHP, and 1341 control infants from 2000 through 2009 at Keio University Hospital and 45 other hospitals throughout Japan (Table 1). All infants were

Table 1. Characteristics of the study subjects.

	C21OHD	PORD	TH17OHP	Control
n	29	9	67	1341
Sex, M/F	20/9	4/5	44/23	759/582
Median gestational age, weeks (range)	38 (31–41)	40 (37–41)	37 (26–41)	38 (22–42)
Median age at analysis, days (range)	11 (0–45)	59 (3–146)	35 (3–164)	4 (0–180)
Median birth weight, g (range)	3060 (1464–4030)	2818 (2330–3066)	2670 (895–4980)	2878 (442–4506)

Japanese, with ages between 0–180 days. The diagnosis of C21OHD and PORD was confirmed by *CYP21A2* and *POR* gene analysis, respectively (Table 2). The diagnosis of TH17OHP was made in the neonates fulfilling all the following criteria; (*a*) 17OHP concentration in the dried blood spot mass screening program in Japan (direct ELISA assay), (*b*) blood 17OHP concentration confirmed to be normal by repeated measure-

Table 2. Genotypes of 29 subjects with C21OHD and 9 with PORD.

Patients	Sex	Gestational age, weeks	Copy 1	Copy 2
C21OHD				
1, 2, 3	M	36, 36, 40	Del or conv[a]	Del or conv
4, 5	M	38, 39	Del or conv	R356W
6	M	38	Del or conv	E6 cluster
7	M	40	Del or conv	L307+T
8, 9	M	38, 40	Del or conv	I2 splicing
10	M	41	Del or conv	I172N
11	M	38	Del or conv	I78 mol/L
12	M	38	Δ8bp[d]	Q318X
13, 14	M	38, 39	R356W	I2 splicing
15	M	38	E6 cluster	I2 splicing
16	M	38	I2 splicing	I2 splicing
17, 18	M	35, 39	I2 splicing	I172N
19	M	35	I172N	I172N
20	M	39	Del or conv, I172N	Δ8bp, I2 splicing
21, 22	F	38, 40	Del or conv	Del or conv
23	F	31	Del or conv	Δ8bp
24	F	39	Del or conv	I172N
25	F	38	R356W	R356W
26, 27	F	37, 38	I2 splicing	I2 splicing
28, 29	F	35, 39	I2 splicing	I172N
PORD				
1,2	M	38, 40	R457H	R457H
3	M	37	R457H	Q555fsX611
4	M	40	R457H	A462 S463insIA
5, 6, 7, 8	F	37, 39, 40, 40	R457H	R457H
9	F	41	R457H	E580Q

[a] Del or conv, deletion or large gene conversion; E6 cluster, cluster of mutations (I236D, V237E, M239K) in exon 6; I2 splicing, intron 2 −13 A/C>G; Δ8bp, 8-bp deletion in exon 3.

ments [ELISA assay (direct or extraction method) or RIA], and (*c*) consistently good overall general condition. Any subjects with abnormal physical findings were excluded. The control infants were without neurologic and endocrinologic abnormalities, and none of the subjects received antenatal or perinatal glucocorticoid before urine sampling. Table 1 shows characteristics of the study subjects.

Spot urine samples were randomly collected for the study and kept at −20 °C until analysis. We studied each infant for urinary steroid profile by GC-MS/selected ion monitoring (GC-MS-SIM), as reported *(8)* with minor modification. In brief, 0.05- to 0.2-mL urine samples were subjected enzymatic hydrolysis and organic solvent extraction and methyloxime-trimethylsilyl derivatized, and the derivative was subjected to GC-MS-SIM analysis. GC-MS-SIM analysis was performed on an HP5890II GC with an HP-Ultra1 fused silica column (25 m × 0.2 nm × 0.33 μm) coupled to an HP5971MS (Agilent Technologies). We quantified each steroid with stigmasterol as the internal standard. The turnaround time of the assay is 2 days.

We measured Ptl and the cortisol metabolites 5α-tetrahydrocortisone and 5β-tetrahydrocortisone (sum of these metabolites termed THEs) and calculated the ratio of Ptl to the cortisol metabolites (Ptl/THEs) *(5, 9)* to differentiate C21OHD and PORD from TH17OHP and controls. Ptl was considered to be equal to 0.001 mg/g creatinine for calculation in infants whose Ptl was under the detection limit (<0.001 mg/g creatinine). We measured metabolites of 3 steroids, namely dehydroepiandrosterone (DHEA), androstenedione (AD4), and 11β-hydroxyandrostenedione (11OHAD4), and calculated the sum of DHEA metabolites (DHEA, androstenediol, 16α-hydroxy-DHEA, 16β-hydroxy-DHEA, 16-oxo-androstenediol, and androstenetriol), the sum of AD4 metabolites (androsterone and etiocholanolone) *(8, 10)*, and the 11OHAD4 metabolite (11HA). (11β-Hydroxyetiocholanolone could not be measured in newborns, as described *(8)*.) The above sum of DHEA metabolites have been reported to include approximately 70% of DHEA metabolites in newborns *(11)*. The above sum of AD4 metabolites are defined as androgen metabolites because, whereas these 2 steroids are metabolites of AD4, they are also the metabolites of testosterone and dihydrotestosterone in boys. Androgen metabolites are analyzed separately by sex, since male androgen metabolites in this age group are increased from testicular-derived androsterone and etiocholanolone.

We measured urinary creatinine by IATRO-LQ CRE (A)II (Mitsubishi Chemical Medience Co.) and expressed urinary steroid concentration relative to urinary creatinine (mg/g creatinine).

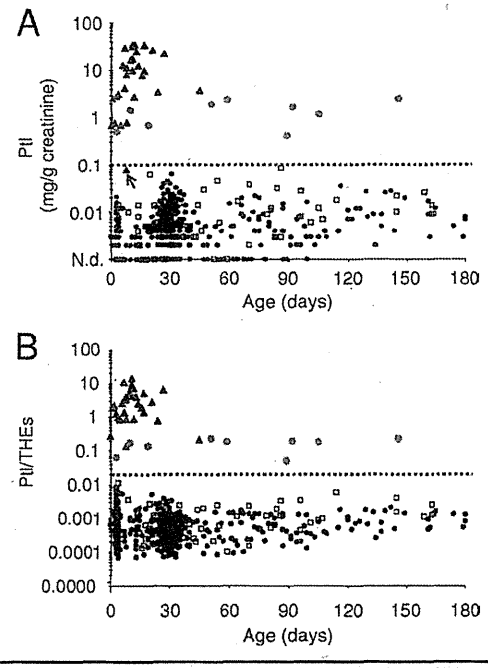

Fig. 2. Urinary (A) Ptl and Ptl/THEs (B) in infants with C21OHD, PORD, TH17OHP, and controls.

Dashed lines show cutoff: Ptl, 0.1 mg/g creatinine; Ptl/THEs, 0.020. ▲, C21OHD; ●, PORD; □, TH17OHP; ●, control. An arrow points to the patient with C21OHD at a lower Ptl value than the cutoff. N.d., not detected.

Statistical analysis of DHEA, androgen, and 11OHAD4 metabolites was carried out by Mann–Whitney *U*-test between C21OHD and PORD. A *P* value of <0.05 was considered statistically significant.

Results

DIFFERENTIATION OF C21OHD AND PORD FROM TH17OHP AND CONTROLS

Fig. 2 shows the results of urinary Ptl and Ptl/THEs. Ptl [median (range) mg/g creatinine] was 10 (0.079–36) in C21OHD, 1.5 (0.42–2.6) in PORD, 0.006 (<0.001–0.086) in TH17OHP, and <0.001 (<0.001–0.064) in controls. Ptl/THEs was 2.5 (0.14–15) in C21OHD, 0.18 (0.051–0.23) in PORD, 0.00083 (0.00010–0.011) in TH17OHP, and 0.00038 (0.000068–0.0083) in controls. Ptl differentiated C21OHD and PORD from TH17OHP and controls with 96.9% (95% CI 91.6%–97.4%) sensitivity and 100% (99.8%–100%) specificity with cutoff 0.1 mg/g creatinine. All patients with TH17OHP and controls showed Ptl concentrations below the cutoff. An 8-day-old patient with C21OHD whose birth weight was 1628 g had a lower Ptl value

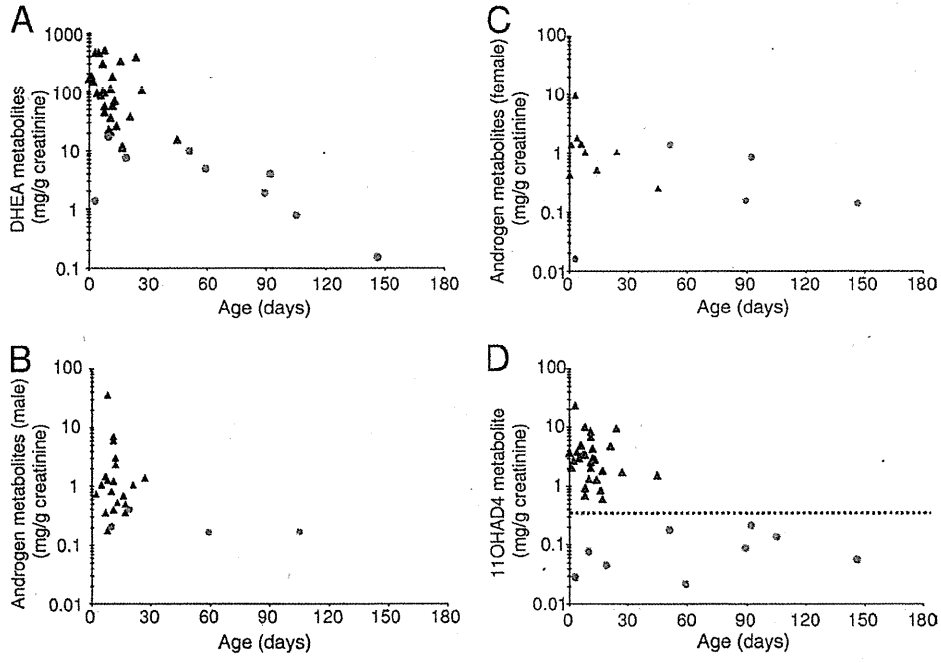

Fig. 3. Urinary metabolites of 17,20-lyase products DHEA (A), androgen (male) (B), androgen (female) (C), and 11OHAD4 (D) in infants with C21OHD and PORD.

Dashed line in (D) shows cutoff of 0.35 mg/g creatinine for 11OHAD4 metabolite. ▲, C21OHD; ●, PORD.

than the cutoff (Fig. 2A, arrow). Ptl/THEs differentiated C21OHD and PORD from TH17OHP and control with 100% (95.1%–100%) diagnostic sensitivity and 100% (99.8%–100%) diagnostic specificity with the 0.020 cutoff.

DISCRIMINATION BETWEEN C21OHD AND PORD

Fig. 3 shows the results of urinary metabolites of 17,20-lyase products (mg/g creatinine) in C21OHD and PORD. DHEA metabolites were 97 (11–505) in C21OHD and 4.0 (0.15–17) in PORD. Androgen metabolites were, for boys, 1.1 (0.18–36) in C21OHD and 0.19 (0.17–0.41) in PORD, and for girls, 1.1 (0.26–9.9) in C21OHD and 0.16 (0.016–1.4) in PORD. 11OHAD4 metabolite was 3.0 (0.61–24) in C21OHD and 0.077 (0.022–0.22) in PORD. All metabolites of 17,20-lyase products showed significant differences between C21OHD and PORD (DHEA metabolites, $P < 0.001$; androgen metabolites (male), $P = 0.006$; androgen metabolites (female), $P = 0.039$; 11OHAD4 metabolite, $P < 0.001$). 11OHAD4 metabolite (11HA) discriminated between C21OHD and PORD with 100% (94.2%–100%) diagnostic sensitivity and 100% (81.4%–100%) diagnostic specificity with the 0.35 mg/g creatinine cutoff. Urinary DHEA and androgen metabolites showed overlap between C21OHD and PORD.

Discussion

We established a 2-step biochemical differential diagnosis for C21OHD and PORD by urinary steroid profile. First, by using a specific cutoff of the ratio of Ptl to THEs, we were able to differentiate C21OHD and PORD from TH17OHP and controls. Second, by using a specific cutoff of 11HA, we were able to distinguish between C21OHD and PORD. Although a distinctive steroid excretion pattern in C21OHD and PORD had been reported *(3, 5, 6)*, no clear cutoff of urinary steroid metabolites was reported in any ages to discriminate between C21OHD and PORD. To the best of our knowledge, this is the first report of a cutoff for biochemical differential diagnosis of C21OHD and PORD in infants. As for TH17OHP, an adequate observation period and timing for repeat blood test are as yet unknown. It is difficult to differentiate between C21OHD and PORD by current standard hormonal testing and clinical observation *(3, 4)*. This 2-step method can diagnose TH17OHP, C21OHD, and PORD by 1 as-

say with a noninvasive spot urine sample while infants have increased concentrations of serum 17OHP.

Increased Ptl and Ptl/THEs in C21OHD and PORD must reflect the impaired activity of 21-hydroxylase. We showed that a specific cutoff of Ptl/THEs differentiated C21OHD and PORD from TH17OHP and controls with no overlap. In patients with C21OHD, impaired activity of 21-hydroxylase led to an increase in the precursor steroid 17OHP. As a result, Ptl, which is a metabolite of 21DOF, was increased. Because the activity of 21-hydroxylase in patients with PORD was impaired by less electron supply from POR, increased Ptl was reasonable.

Decreased 11HA in PORD must reflect the impaired activity of 17,20-lyase. The reason is unclear why the urinary 11OHAD4 metabolite was the only 1 among other metabolites of 17,20-lyase products that showed a difference between C21OHD and PORD, but the reason is probably that 11OHAD4 is of purely adrenal origin. DHEA metabolites showed tiny overlap between C21OHD and PORD that may derive from unexpectedly low DHEA metabolites in 3 patients with C21OHD. On the 1 hand, androgen metabolites showed a clear overlap that can be explained by androgen production in the backdoor pathway (Fig. 1, dashed arrow), which is proven in the tammar wallaby *(12)* and postulated in the human newborn *(13)*. Androsterone can be derived not only from AD4 and dihydrotestosterone in the conventional pathway but also from 5α-pregnane-3α,17α-diol-20-one in the backdoor pathway *(12, 13)*. In PORD, androsterone could increase during early infancy *(13)*, resulting in overlap in androgen metabolites.

One may argue that PD, the ratio of PD to 17,20-lyase metabolites (e.g., 11HA, DHEA metabolites), or the ratio of 17α-hydroxypregnenolone metabolite to DHEA metabolites *(13)* is discriminatory (Fig. 1). Unfortunately, the measurement of PD is sometimes problematic in our GC-MS method in newborns and we cannot calculate the concentration or the ratio. We have reported that the ratio of 17α-hydroxypregnenolone metabolites to DHEA metabolites discriminated 22 patients with PORD from healthy infants *(13)*, whereas this ratio could not discriminate C21OHD and PORD completely in this cohort (data not shown).

This study had 4 limitations. First, nonclassic 21OHD was not included in study subjects. Nonclassic 21OHD is known to have lower blood 17OHP than C21OHD *(14, 15)*. Thus, it is conceivable that these individuals have lower Ptl/THEs and 11HA than C21OHD. Further studies are required to determine if the same cutoff can discriminate between nonclassic 21OHD and PORD. Second, the total number of affected infants, and specifically the number of very-low-birthweight infants (only 2), was limited in this study. Infants born with very low birthweight should have less hepatic enzyme activities such as 5β-reductase, 3α-hydroxysteroid dehydrogenase, and 20α-hydroxysteroid dehydrogenase, leading to less conversion of 21DOF to Ptl. Indeed, 1 patient with C21OHD who was born with low birthweight had a lower Ptl value than the cutoff. The third limitation is the random time at which urine samples were collected, although it is known that steroid metabolism starts to show diurnal variation around 2–3 months of age *(16)*. We unintentionally proved that we could use the urine sample whenever it is collected. As for the fourth limitation, our data in Japanese infants may not apply to other ethnic populations. Enzymatic residual activity in PORD has been reported to differ depending on genotype *(17)*. The common mutation was R457H in Japanese PORD *(7, 18)* and A287P in whites *(19)*. R457H has 1%–3% supporting activity for 17α-hydroxylase and virtually no activity for 17,20-lyase compared to wild type, whereas A287P has 40% activity for 17α-hydroxylase and about 20% for 17,20-lyase *(17, 19, 20)*. In fact, all subjects with PORD were Japanese with homozygous or heterozygous R457H mutation (Table 2). For PORD cohorts with higher 17,20-lyase activity (i.e., A287P), 11HA might not be as useful. Thus other cutoffs may be required for non-Japanese.

In conclusion, we demonstrated a 2-step biochemical differential diagnosis for C21OHD and PORD by urinary steroid metabolites such as Ptl, THEs, and 11HA. We believe that this 2-step biochemical diagnosis would be valuable for Japanese infants whose clinical differential diagnosis is difficult.

Author Contributions: *All authors confirmed they have contributed to the intellectual content of this paper and have met the following 3 requirements: (a) significant contributions to the conception and design, acquisition of data, or analysis and interpretation of data; (b) drafting or revising the article for intellectual content; and (c) final approval of the published article.*

Authors' Disclosures or Potential Conflicts of Interest: *Upon manuscript submission, all authors completed the Disclosures of Potential Conflict of Interest form. Potential conflicts of interest:*

Employment or Leadership: None declared.
Consultant or Advisory Role: None declared.
Stock Ownership: None declared.
Honoraria: None declared.
Research Funding: Funded by Health and Labor Sciences Research Grants for the Research on Intractable Disease from Ministry of Health, Labor, and Welfare in Japan; Grants-in-Aid for Scientific Research from the Japan Society for the Promotion of Science; and a Grant-in-Aid for Scientific Research on Innovative Areas from the Ministry of Education, Culture, Sports, Science, and Technology.
Expert Testimony: None declared.

Role of Sponsor: The funding organizations played no role in the design of study, choice of enrolled patients, review and interpretation of data, or preparation or approval of manuscript.

Acknowledgments: We thank Dr. Makoto Anzo, Dr. Katsumi Goji, Dr. Keiichi Hara, Dr. Kazunori Sanayama, Dr. Kazuhiro Mori, Dr. Keisuke Nagasaki, Dr. Shinji Nomura, Dr. Makoto Ono, Dr. Nobutaka Sasaki, Dr. Kimihira Seki, Dr. Eri Suzuki, Dr. Ikuko Takahashi, Dr. Noriyuki Takubo, Dr. Shiho Tamaura, and Dr. Etsushi Tsuchida for giving us valuable case samples. We also thank Dr. Misa Honda for critical comments and language editing.

References

1. Nimkarn S, Lin-Su K, New MI. Steroid 21 hydroxylase deficiency congenital adrenal hyperplasia. Endocrinol Metab Clin North Am 2009;38: 699–718.
2. Miller WL. P450 oxidoreductase deficiency: a new disorder of steroidogenesis with multiple clinical manifestations. Trends Endocrinol Metab 2004; 15:311–5.
3. Fukami M, Hasegawa T, Horikawa R, Ohashi T, Nishimura G, Homma K, Ogata T. Cytochrome P450 oxidoreductase deficiency in three patients initially regarded as having 21-hydroxylase deficiency and/or aromatase deficiency: diagnostic value of urine steroid hormone analysis. Pediatr Res 2006;59:276–80.
4. Stewart PM. The adrenal cortex. In: Larsen PR, Kronenberg HM, Melrned S, Polonsky KS (eds) Williams textbook of endocrinology, 10th ed. Philadelphia: Saunders 2002;491–551.
5. Homma K, Hasegawa T, Takeshita E, Watanabe K, Anzo M, Toyoura T, et al. Elevated urine pregnanetriolone definitively establishes the diagnosis of classical 21-hydroxylase deficiency in term and preterm neonates. J Clin Endocrinol Metab 2004;89:6087–91.
6. Shackleton C, Marcos J, Malunowicz EM, Szarras-Czapnik M, Jira P, Taylor NF, et al. Biochemical diagnosis of Antley-Bixler syndrome by steroid analysis. Am J Med Genet A 2004;128:A223–31.
7. Fukami M, Nishimura G, Homma K, Nagai T, Hanaki K, Uematsu A, et al. Cytochrome P450 oxidoreductase deficiency: identification and characterization of biallelic mutations and genotype-phenotype correlations in 35 Japanese patients. J Clin Endocrinol Metab 2009;94: 1723–31.
8. Homma K, Hasegawa T, Masumoto M, Takeshita E, Watanabe K, Chiba H, et al. Reference values for urinary steroids in Japanese newborn infants: gas chromatography/mass spectrometry in selected ion monitoring. Endocr J 2003;50:783–92.
9. Caulfield MP, Lynn T, Gottschalk ME, Jones KL, Taylor NF, Malunowicz EM, et al. The diagnosis of congenital adrenal hyperplasia in the newborn by gas chromatography/mass spectrometry analysis of random urine specimens. J Clin Endocrinol Metab 2002;87:3682–90.
10. Wudy SA, Hartmann MF. Gas chromatography-mass spectrometry profiling of steroids in times of molecular biology. Horm Metab Res 2004;36: 415–22.
11. Shackleton CH, Honour JW, Taylor NF. Metabolism of fetal and neonatal adrenal steroids. J Steroid Biochem 1979;11:523–9.
12. Wilson JD, Auchus RJ, Leihy MW, Guryev OL, Estabrook RW, Osborn SM, et al. 5alpha-Androstane-3alpha,17beta-diol is formed in tammar wallaby pouch young testes by a pathway involving 5alpha-pregnane-3alpha,17alpha-diol-20-one as a key intermediate. Endocrinology 2003;144:575–80.
13. Homma K, Hasegawa T, Nagai T, Adachi M, Horikawa R, Fujiwara I, et al. Urine steroid hormone profile analysis in cytochrome P450 oxidoreductase deficiency: implication for the backdoor pathway to dihydrotestosterone: J Clin Endocrinol Metab 2006;91:2643–9.
14. New MI. Extensive clinical experience: nonclassical 21-hydroxylase deficiency. J Clin Endocrinol Metab 2006;91:4205–14.
15. Kashimada K, Ono M, Onishi T, Koyama S, Toyoura T, Imai K, et al. Clinical course of patients with nonclassical 21-hydroxylase deficiency (21-OHD) diagnosed in infancy and childhood. Endocr J 2008;55:397–404.
16. Custodio RJ, Junior CE, Milani SL, Simões AL, de Castro M, Moreira AC. The emergence of the cortisol circadian rhythm in monozygotic and dizygotic twin infants: the twin-pair synchrony. Clin Endocrinol (Oxf) 2007;66:192–7.
17. Miller WL, Huang N, Agrawal V, Giacomini KM. Genetic variation in human P450 oxidoreductase. Mol Cell Endocrinol 2009;300:180–4.
18. Fukami M, Horikawa R, Nagai T, Tanaka T, Naiki Y, Sato N, et al. Cytochrome P450 oxidoreductase gene mutations and Antley-Bixler syndrome with abnormal genitalia and/or impaired steroidogenesis: molecular and clinical studies in 10 patients. J Clin Endocrinol Metab 2005;90: 414–26.
19. Huang N, Pandey AV, Agrawal V, Reardon W, Lapunzina PD, Mowat D, et al. Diversity and function of mutations in p450 oxidoreductase in patients with Antley-Bixler syndrome and disordered steroidogenesis. Am J Hum Genet 2005;76: 729–49.
20. Dhir V, Ivison HE, Krone N, Shackleton CH, Doherty AJ, Stewart PM, Arlt W. Differential inhibition of CYP17A1 and CYP21A2 activities by the P450 oxidoreductase mutant A287P. Mol Endocrinol 2007;21:1958–68.

OPEN ACCESS Freely available online PLoS one

Screening of *MAMLD1* Mutations in 70 Children with 46,XY DSD: Identification and Functional Analysis of Two New Mutations

Nicolas Kalfa[1,2], Maki Fukami[3], Pascal Philibert[1], Francoise Audran[1], Catherine Pienkowski[4], Jacques Weill[5], Graziella Pinto[6], Sylvie Manouvrier[7], Michel Polak[6], Totsumo Ogata[3], Charles Sultan[1,2,8]*

1 Service d'Hormonologie, Hôpital Lapeyronie, CHU de Montpellier et UM1, Montpellier, France, **2** Service de Chirurgie et Urologie Pédiatrique, Hôpital Lapeyronie, CHU de Montpellier et UM1, Montpellier, France, **3** Department of Molecular Endocrinology, National Research Institute for Child Health and Development, Tokyo, Japan, **4** Unité d'Endocrinologie Pédiatrique, Hôpital des Enfants, CHU de Toulouse, Toulouse, France, **5** Clinique de Pédiatrie, Hôpital Jeanne de Flandre, CHU de Lille, Lille, France, **6** Unité d'Endocrinologie Pédiatrique, Hôpital Necker Enfants Malades, APHP, Paris, France, **7** Service de Génétique Clinique, Hôpital Jeanne de Flandre, CHU de Lille, Lille, France, **8** Unité d'Endocrinologie et Gynécologie Pédiatriques, Service de Pédiatrie, Hôpital Arnaud de Villeneuve et UM1, CHU de Montpellier, Montpellier, France

Abstract

More than 50% of children with severe 46,XY disorders of sex development (DSD) do not have a definitive etiological diagnosis. Besides gonadal dysgenesis, defects in androgen biosynthesis, and abnormalities in androgen sensitivity, the Mastermind-like domain containing 1 (*MAMLD1*) gene, which was identified as critical for the development of male genitalia, may be implicated. The present study investigated whether *MAMLD1* is implicated in cases of severe 46,XY DSD and whether routine sequencing of *MAMLD1* should be performed in these patients. Seventy children with severe non-syndromic 46,XY DSD of unknown etiology were studied. One hundred and fifty healthy individuals were included as controls. Direct sequencing of the *MAMLD1, AR, SRD5A2* and *NR5A1* genes was performed. The transactivation function of the variant *MAMLD1* proteins was quantified by the luciferase method. Two new mutations were identified: p.S143X (c.428C>A) in a patient with scrotal hypospadias with microphallus and p.P384L (c.1151C>T) in a patient with penile hypospadias with microphallus. The *in vitro* functional study confirmed no residual transactivating function of the p.S143X mutant and a significantly reduced transactivation function of the p.P384L protein ($p = 0.0032$). The p.P359S, p.N662S and p.H347Q variants are also reported with particularly high frequency of the p.359T- p.662G haplotype in the DSD patients. Severe undervirilization in XY newborns can reveal mutations of *MAMLD1*. *MAMLD1* should be routinely sequenced in these patients with otherwise normal *AR, SRD5A2* and *NR5A1*genes.

Citation: Kalfa N, Fukami M, Philibert P, Audran F, Pienkowski C, et al. (2012) Screening of *MAMLD1* Mutations in 70 Children with 46,XY DSD: Identification and Functional Analysis of Two New Mutations. PLoS ONE 7(3): e32505. doi:10.1371/journal.pone.0032505

Editor: Irina Agoulnik, Florida International University, United States of America

Received November 7, 2011; **Accepted** January 31, 2012; **Published** March 30, 2012

Funding: This study was funded by a Programme Hospitalier de Recherch Clinique Inter-Régional (PHRC number UF 8270) provided by CHU de Montpellier and by a grant from Fondation pour la Recherche Médicale FRM110309. The funders had no role in study design, data collection and analysis, decision to publish, or preparation of the manuscript.

Competing Interests: The authors have declared that no competing interests exist.

* E-mail: c-sultan@chu-montpellier.fr

Introduction

The disorders of sex development (DSD) comprise a variety of anomalies defined by congenital conditions in which chromosomal, gonadal, or anatomical sex is atypical. The prevalence of the 46,XY disorders of sex development (46,XY DSD) is difficult to determine with accuracy because of the heterogeneity in the clinical presentation and the etiologies. The estimated incidence of severe 46,XY DSD with uncertain sex is 2.2 per 10,000 births [1], and for a minor form of 46,XY DSD with isolated and non-severe hypospadias, the incidence is estimated at 1 in 250–400 births [2]. Two independent surveillance systems in the United States, the nationwide Birth Defects Monitoring Program (BDMP) and the Metropolitan Atlanta Congenital Defects Program (MACDP), reported a near doubling in the hypospadias rate in comparison with the immediately preceding decades [3]. Although recent studies have questioned this reported rise and provide conflicting data [4,5], the elucidation of the pathophysiology of these genital malformations remains challenging.

The etiologies of 46,XY DSD are usually gonadal dysgenesis (defect in *SRY* and downstream genes such as *SOX9, WT1, NR5A1* [6,7], etc.), defects in androgen biosynthesis and, more frequently, abnormalities in androgen sensitivity. Unfortunately, more than 50% of children with severe 46,XY DSD presenting with uncertain sex do not have a definitive clinical diagnosis [8]. For instance, an *AR* gene defect is identified in less than 10% of the cases [9].

In addition to these well classified causes, a recent candidate gene was identified as critical for the development of male genitalia: the Mastermind-like domain containing 1 (*MAMLD1*) gene (formerly *CXorf6*). This gene was discovered during studies to find the gene responsible for X-linked myotubular myopathy, *MTM1*, which maps to proximal Xq28 [10]: *MAMLD1* was observed to be deleted in patients with both the myopathy and external genital malformations [10,11,12]. Polymorphisms of *MAMLD1* have been reported in patients with isolated hypospadias, the less severe form of 46,XY DSD, but these variants usually

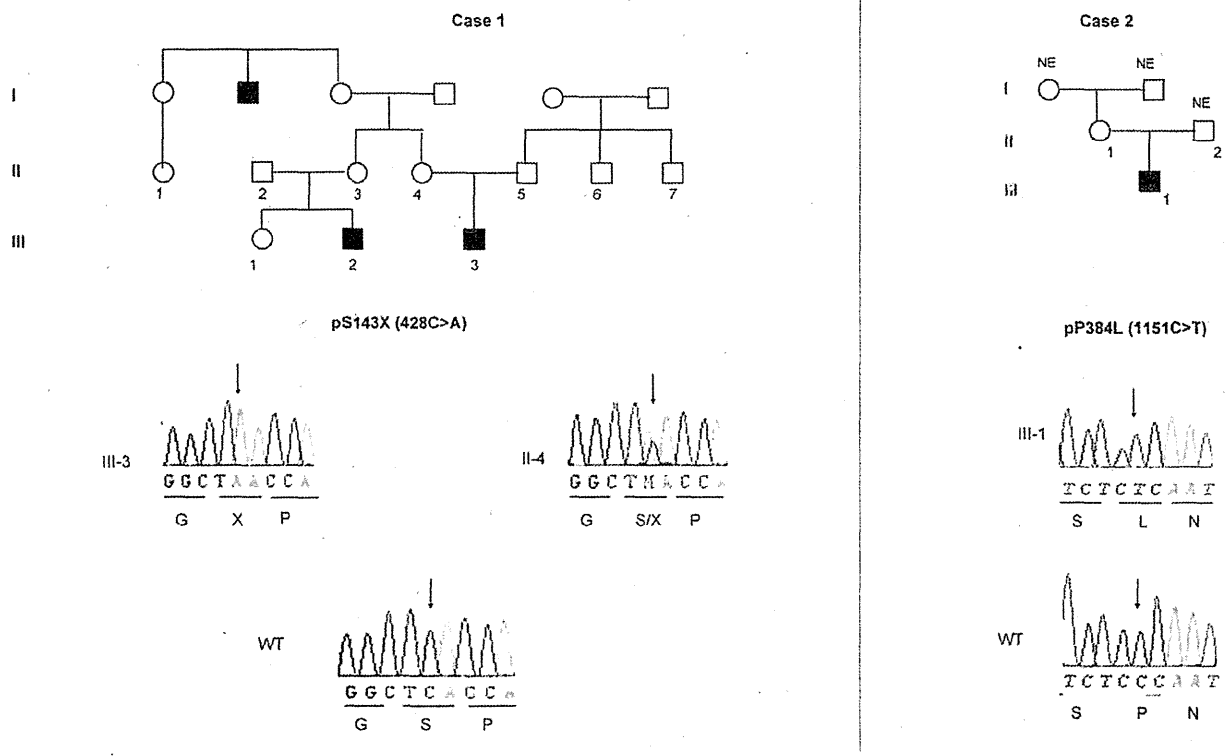

Figure 1. Electrochromatograms and pedigrees of the three patients with *MAMLD1* mutations. The black squares indicate patients with posterior hypospadias. All mutant sequences were controlled by wildtype (WT) DNA. Regarding case 1's family, only the members III-3 and II-4 were genotyped, as the other members in the pedigree declined genetic testing.
doi:10.1371/journal.pone.0032505.g001

do not affect the transactivation of the protein [13,14]. Conversely, severe 46,XY DSD with uncertain sex has been sparsely studied. To date, only one study has focused on these patients: Fukami et al. identified three nonsense mutations in four individuals from a group of 166 patients [15]. The aim of the present study was to determine whether *MAMLD1* is frequently implicated in newborns and children with severe 46,XY DSD with uncertain sex and whether *MAMLD1* should be routinely sequenced in these patients.

Materials and Methods

Patients and controls

Two hundred and twenty individuals were included in this study. Seventy children presented with non-syndromic 46,XY DSD of unknown etiology. According to the Quigley classification [16], 8 patients exhibited a stage 2 phenotype; 32 patients, stage 3; 20 patients, stage 4; 5 patients, stage 5; and 5 patients, stage 6. One hundred and fifty healthy individuals were included as controls. Controls were chosen among patients without urinary, genital, or endocrine disease, or any other congenital malformation. For instance, patients with acute appendicitis or operated on for circumcision without phimosis were included. This study was approved by the Institutional Review Board (CPP-Montpellier, ID RCB No. 2008-A00781-54). Written consent was obtained from the parents, carers or guardians on behalf of the participating minors. When a mutation was identified, other family members were examined if possible. The patients and controls were Caucasian.

DNA extraction

DNA was extracted from peripheral blood using a QIAamp DNA blood minikit (Qiagen, Courtaboeuf, France).

Mutational analysis of MAMLD1

Direct sequencing of *MAMLD1* coding exons and their flanking splice sites was performed in all patients and controls using primers as previously described [17]. The 3730xl DNA Analyzer (Applied Biosystems, Foster City, CA, USA) was used. Sequencing reactions were repeated twice with at least two different PCR products. The DNA sequences were compared with the sequences of normal controls and the reference genomes from the ensembl.org database (Ensembl: ENSG00000013619) and the genebank database (MIM: 300120, NCBI Gene ID: 10046). It is notable that the number of the cDNA and amino acids has been changed recently because of the recognition of a novel *MAMLD1* start codon. This report describes *MAMLD1* cDNA and amino acids according to the new system.

Molecular analysis of androgen sensitivity

A molecular analysis of the androgen receptor (*AR*) and 5 alpha reductase type 2 (*SRD5A2*) genes was performed in all patients.

Table 1. Clinical and hormonal data of patients with mutated *MAMLD1*.

Patient	Case 1	Case 2
MAMLD1 mutation	pS143X	pP384L
Previous medical history	None	Maternal diabetes
Genital phenotype		
Urethral meatus	Scrotal	Penile posterior
Age at exam (yr,mo)	0,0	0,0
Microphallus	Yes, 20 mm	Yes, 20 mm with cuvature
Testis position	Intra-scrotal	Intra-scrotal
Testis size (normal = 1–2 ml)	Normal	Normal
Scrotal appearance	Ventral transposition, Bifid Scrotum	Bifid Scrotum
Renal and urinary tract structure	Normal	Normal
Extragenital phenotype	Normal	Normal
Growth		
Birth height, cm (SDS)	51 (+0)	50.5 (+0)
Birth weight, Kg (SDS)	3.540 (+0)	3.750 (+0.5)
Serum hormone level		
Time of measurment (yr,mo)	0,0	0,3
Testosterone (ng/ml) (1–3 ng/ml)	1.78	<0.07
LH (UI/l) (1–12 UI/l)	10	0.3
FSH (UI/l) (1–10 UI/l)	0.8	0.8
AMH	336 ng/ml	19 ng/ml*
Inhibin	NA	<15 ng/ml*

SD: standard deviation. ND: not determined. NA: not available. DHT: dihydrotestosterone. DHEA: dihydroepiandrsosterone. Parentheses indicate the standard deviation for height and weight and the normal range for hormone serum levels. Testes of 1–2 ml can be regarded as normal, as recently reported by Shibata et al. [34].
*It is notable that anti-mullerian hormone and inhibin were lowered in one case. *MAMLD1* is indeed reported to be expressed in Sertoli cells, as well [15].
doi:10.1371/journal.pone.0032505.t001

Exons 1–8 of the *AR* gene were amplified by PCR using sets of primers and reactions previously described [18]. Molecular analysis of the *SRD5A2* gene (exons 1–5) was performed as previously reported [19]. PCRs were verified for correct length on agarose gel, purified with Qiaquick PCR columns (Qiagen), and sequenced with the ABI Prism Big Dye terminator sequencing kit. *NR5A1*was sequenced in 46,XY DSD children with low plasma testosterone as previously published [6,20].

Homology study

Ensembl.org detected the putative homologs of the human *MAMLD1* gene and alignments were made with the ClustalW software at http://www.ebi.ac.uk/Tools/msa/clustalw2/.

Structure prediction

The potential impact of variants was first predicted using X *in-silico* tools for secondary structure, tertiary structure and prediction of the consequences of amino acid changes.

The secondary structure for wildtype and variants was predicted using JPred software [21] (http://www.compbio.dundee.ac.uk/www-jpred/). The relative accessibility of amino acids was studied with Netsurf software [22] (http://www.cbs.dtu.dk/services/NetSurfP/). The three-dimensional structure was predicted by the Protein Homology/analogY Recognition Engine (PhyreEngine) from the Structural Bioinformatics Group, Imperial College, London, at http:www.sbg.bio.ic.ac.uk/phyrew/. This tool can detect remote homologous proteins with similar tertiary structures, based on multiple sequence profiles with structure-based profiles [23].

The functional consequences of amino acid changes were predicted using four algorithms. Polyphen (Harvard, USA) [24,25], Panther [26], Sift (University of British Columbia) [27] and SNP-3D (University of Maryland) [28] were used, respectively, at http://genetics.bwh.harvard.edu/pph/, http://www.pantherdb.org/tools/csnpScoreForm.jsp., http://sift.jcvi.org/, and http://www.snps3d.org/modules.php?name=Search&op=advanced%20search. These algorithms are based on the alignment of orthologous and/or paralogous protein sequences and/or structural constraints.

Transactivation analysis of MAMLD1

The transactivation function of the variant MAMLD1 proteins was analyzed by the luciferase method [29]. We used the previously reported luciferase reporter vector containing the promoter sequence of mouse hairy/enhancer of split 3 (*Hes3*) (−2,715~+261 bp) [30] and expression vectors containing cDNAs for wildtype *MAMLD1*, p.S143X and p.P384L [29]. Mouse Leydig tumor (MLTC1) cells (ATCC, CRL-2065) seeded in 12-well dishes ($0.5–1.0\times10^5$ cells/well) were transiently transfected using Lipofectamine 2000 (Invitrogen) with 0.6 μg of luciferase reporter vector and 0.6 μg of expression vector for wildtype or variant *MAMLD1*, together with 20 ng of pRL-CMV vector (Promega) used as an internal control. As a control for the expression vectors, an empty counterpart vector was transfected. Luciferase assays performed with a Lumat LB9507 (Berthold) 48 hours after transfection were repeated three times.

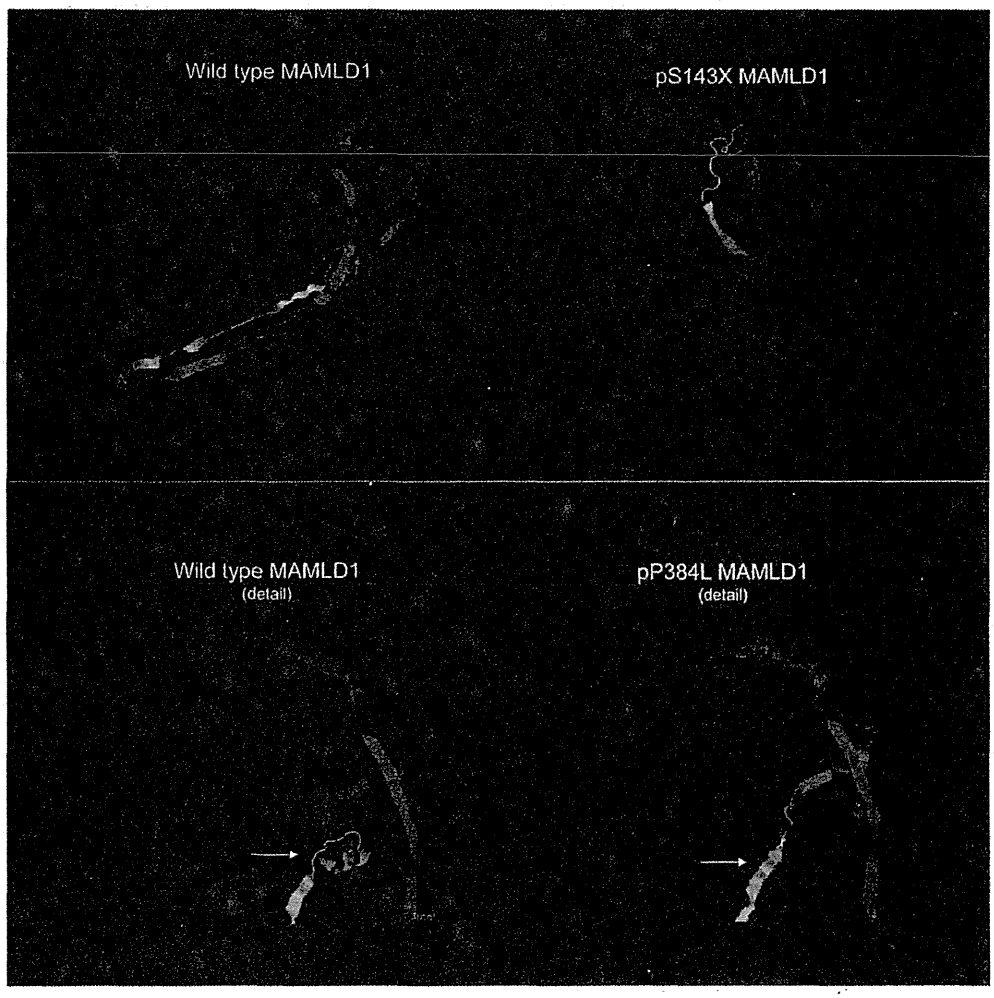

Figure 2. Tertiary structure prediction of the wildtype protein (left column) and with the mutants. 3D structure was predicted at Protein Homology/analogY Recognition Engine (PhyreEngine) from the Structural Bioinformatics Group, Imperial College, London, at http:www.sbg.bio.ic.ac.uk/phyre~/. The plain arrows show the changes in the shape of the protein between the wildtype and p.P384L.
doi:10.1371/journal.pone.0032505.g002

Statistical methods

Haplotype frequencies were compared between cases and controls using the χ^2 test and the Fisher test on SPSS 16.0 software. The odds ratio (OR) was also considered with the logit confidence intervals method: $OR-CI=e^{LN(OR)\pm 1.96\left(\frac{1}{A}+\frac{1}{B}+\frac{1}{C}+\frac{1}{D}\right)^{0.5}}$. Hapmap and ensembl.org were used to exclude linkage disequilibrium. Regarding the transactivation analysis of *MAMLD1*, the results are expressed using the mean and SD, and statistical significance was determined by the *t*-test.

Results

Mutations of MAMLD1 and functional analyses

Among the 70 newborns and children with 46,XY DSD, two new mutations were identified in two unrelated patients: p.S143X (c.428C>A) and p.P384L (c.1151C>T) (Fig. 1). The clinical and genetic data are summarized in Table 1. None of these mutations was noted in the control group. The sequences of the *AR*, *SRD5A2* and *NR5A1* genes were normal in these patients.

a- The p.S143X mutation was predicted to cause a short and truncated protein. The *in silico* prediction showed profoundly modified amino acid accessibility and 3D structure. Relative surface accessibility and absolute surface accessibility of the last amino acid changed from 0.248 to 0.834 and from 29.124 to 97.721, respectively. PhyreEngine predicted the loss of any functional site without a residual consensus sequence (no homologous sequence over 5% through whole genome) (Fig. 2). The *in vitro* functional study confirmed no residual transactivating function of the mutant (Fig. 3). Interestingly, a maternal uncle and a maternal cousin of the index case both exhibited severe hypospadias (not available for genetic testing). The mother was indeed heterozygous for the mutation (Fig. 1).

b- The p.P384L mutation was found in a patient with posterior penile hypospadias and microphallus. No cryptrochidism was noted. The secondary structure was predicted to be changed in the next four amino acids. The relative and absolute accessibilities of the amino acid were modified from 0.27 to 0.35 and from 39.07 to 65.25, respectively. The 3D structure prediction of the mutated protein was significantly changed (Fig. 2). All four *in silico*

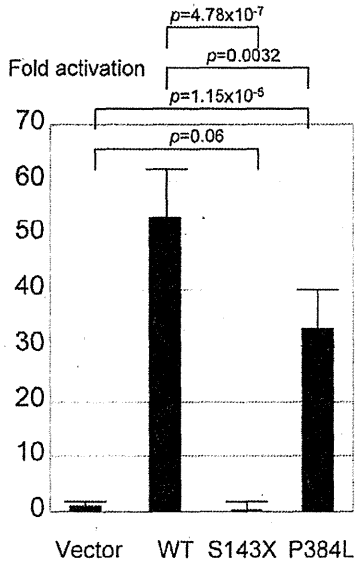

Figure 3. Transactivation function of the variants of the MAMLD1 protein analyzed by the luciferase method. The activity is evaluated for pHes3-luc vector.
doi:10.1371/journal.pone.0032505.g003

algorithms predicted affected protein function (Table 2) with a conserved amino acid throughout species (Table 3). Functional studies confirmed the significantly reduced transactivation function of the p.P384L protein with 60% residual activity when compared with the wildtype protein, $p = 0.0032$ (Fig. 3).

Polymorphisms of MAMLD1

We identified three polymorphisms of *MAMLD1* in our series: p.P359S (c.1075C>T, rs41313406), p.N662S (c.1985A>G, rs2073043) and p.H347Q (c.1041C>A, rs62641609). Regarding the p.P359S and p.N662S polymorphisms, 14 patients exhibited double polymorphisms (S-S haplotype) and five had the p.N359S polymorphism. The phenotypes of the patients with the S-S haplotype were as follows: penile posterior hypospadias and cryptorchidism in three cases, hypospadias and microphallus in five cases (anterior n = 1, penile posterior n = 2 and scrotal hypospadias n = 2), and cryptorchidism and microphallus in six cases (bilateral cryptorchidism n = 5, unilateral cryptorchidism n = 1). Using hapmap and ensembl.org, no linkage disequilibrium was found for these two variants. In previous studies, we and others found that the S-S haplotype was present in only 6/150 controls (4.0%) and 23/360 controls (6.4%) [13,14]. By combining the published series for controls (matched patients and controls), we determined that the incidence of the S-S haplotype was higher in the DSD patients (20%, n = 70 vs. 6%, n = 510, $p = 0.0003$) (OR = 3.86, CI from 1.94 to 7.70, $p = 0.05$). Haplotypes and their relative frequencies in each group of patients are summarized in Table 4.

The p.H347Q variant, previously reported as a polymorphism especially in sub-Saharan populations (rs62641609, http://www.ensembl.org/Homo_sapiens/Variation/Summary?r=X:149638386-149639386;v=rs62641609;vdb=variation;vf=16740729), was identified in a patient with posterior hypospadias and microphallus (25 mm length at birth).

Table 2. Prediction of affected protein function using four algorithms.

Algorithm	pP384L
Polyphen	Probably damaging
	score = 0.961 (sensitivity: 0.71; specificity: 0.93)
Sift	Affect protein function
	Sift score = 0.04
Panther	Probability of deleterious effect = 0.42
	(subPSEC score = −2.7)
SNPS3D	Deleterious
	(svm score = −1.75)

References and online access are indicated in the text. Mathematical calculation of the significance of each score is available online.
doi:10.1371/journal.pone.0032505.t002

Discussion

MAMLD1 is a good candidate to explore in patients with unexplained 46,XY DSD, as it has been shown to be expressed in fetal Leydig cells around the critical period for sex development [15]. The transient knockdown of *MAMLD1* mRNA expression results in significantly reduced testosterone production in mouse Leydig tumor cells [29]. *MAMLD1* is further coexpressed with steroidogenic factor (*NR5A1*), which regulates the transcription of genes involved in sex development, and an *NR5A1* target site was found within the *MAMLD1* gene [29,31]. *MAMLD1* thus seems to have an important role in modulating testosterone production during sex development and is involved in the 46,XY disorders of sex development [32].

Regarding the minor forms of 46,XY DSD with isolated and non-severe hypospadias, mutational studies of *MAMLD1* have identified several polymorphisms in this gene. We reported the following variants in patients with isolated hypospadias: p.P359S, p.V505A, p.N662S and p.604ins3Q [13,17], all of which were recently confirmed as polymorphisms [14]. The p.Q602K mutation was also found in one patient with posterior hypospadias and was predicted to affect the splicing process. An association between isolated hypospadias and the rare haplotype p.P359S-p.N662S is also suspected [13,14].

Table 3. Homology study showed that this amino acid was highly conserved through species for the c.1041C>A and c.1151C>T mutations.

Patient	MSSNTLSGSTLRGS**L**NALLSSMTSSSNAAL
Human-MAMLD1	MSSNTLSGSTLRGS**P**NALLSSMTSSSNAAL
Pig	MSSSSLPGSTLHGS**P**GALLSSGAPSSSSAL
Horse	MSSSNLPGSTLQGS**P**NALLSSMVSGSSAAL
Chimpanzee	MSSNTLSGSTLRGS**P**NALLSSMTSSSNAAL
Mouse	MSSSSLSGSAVQSS**P**NALLSSMAPSSNASL
Rabbit	MAPHSLPGSSLQGS**P**NALLSSMAPNSSGAL
Dog	MASSNLPGSSFQAS**P**NALLASMASASSAGL
Cat	MASGNLPGSAFQGS**P**NALLASMASGSSAAL

doi:10.1371/journal.pone.0032505.t003